ORIGIN OF FOLIATION
IN THE
BARRINGTON PASSAGE PLUTON
SOUTHWEST NOVA SCOTIA

Geoffrey K. Gallant

Submitted in Partial Fulfillment of the requirements
for the Degree of Bachelor of Science, Honours
Dalhousie University, Halifax, Nova Scotia
March 1991

Dalhousie University

Department of Geology
Halifax, Nova Scotia
Canada B3H 3J5
(902) 494-2358

DATE May 7, 1991

AUTHOR Geoffrey K. Gallant

TITLE "Origin of Foliation in the Barrington Passage Pluton Southwest Nova Scotia"

Degree B.Sc. Honours Convocation May Year 1991

Permission is herewith granted to Dalhousie University to circulate and to have copied for non-commercial purposes, at its discretion, the above title upon the request of individuals or institutions.

Distribution License

DalSpace requires agreement to this non-exclusive distribution license before your item can appear on DalSpace.

NON-EXCLUSIVE DISTRIBUTION LICENSE

You (the author(s) or copyright owner) grant to Dalhousie University the non-exclusive right to reproduce and distribute your submission worldwide in any medium.

You agree that Dalhousie University may, without changing the content, reformat the submission for the purpose of preservation.

You also agree that Dalhousie University may keep more than one copy of this submission for purposes of security, back-up and preservation.

You agree that the submission is your original work, and that you have the right to grant the rights contained in this license. You also agree that your submission does not, to the best of your knowledge, infringe upon anyone's copyright.

If the submission contains material for which you do not hold copyright, you agree that you have obtained the unrestricted permission of the copyright owner to grant Dalhousie University the rights required by this license, and that such third-party owned material is clearly identified and acknowledged within the text or content of the submission.

If the submission is based upon work that has been sponsored or supported by an agency or organization other than Dalhousie University, you assert that you have fulfilled any right of review or other obligations required by such contract or agreement.

Dalhousie University will clearly identify your name(s) as the author(s) or owner(s) of the submission, and will not make any alteration to the content of the files that you have submitted.

If you have questions regarding this license please contact the repository manager at dalspace@dal.ca.

Grant the distribution license by signing and dating below.

_____ _____

Name of signatory Date

ABSTRACT

New studies provide insight into the processes producing the penetrative foliation observed in the Barrington Passage Pluton (BPP). Preferred alignment of primary minerals, imbrication of feldspars, preferred alignment of enclaves, schlieren layering, and orientation parallel to the contact suggest a magmatic flow origin for most of the BPP. However, features such as recrystallized quartz and biotite, fractured and rotated feldspars, anastomosing foliations, and `S-C'foliations characterize a gneissic texture present along the western margin of the BPP. Local deformation in the area is the result of a shear zone. A younger norite intrusion occurs within the BPP and has locally deformed the tonalite host. There is resetting of the foliation around the norite body. Deformation including extensive plagioclase alteration, fractured and broken feldspars, and recrystallized and reoriented biotite characterize the BPP rocks near the norite body. Forceful intrusion of the norite produced effects on the BPP similar to those produced upon wall rocks by ballooning plutons. Recrystallized quartz aggregates occur throughout the study area, and align parallel to the foliation. Quartz is the only deformed mineral among the magmatically produced foliation samples. This suggests that solid-state deformation is very slight in the BPP.

Keywords: Foliations, submagmatic, tectonic, solid-state, shear zone, deformation, norite, tonalite, ballooning plutons, syntectonic

Acknowledgments

The author would like to thank Dr. D.B. Clarke for his invaluable contributions and infinite patience in his assistance with this paper, Allen Stark and Steven Hinds for assisting with some of the field work, George O'Reilly for advice and assistance with research material, and Kathy Williams, Roberta Hicks, Melanie Haggart, Darren Stiven, and Kevin Desroches for their help with some of the technical work before the deadline.

Table of Contents

List of Figures

List of Tables

Chapter 1

Introduction

1.1 Introduction

The Barrington Passage Pluton (BPP), a biotite tonalite intrusion (Rogers and Barr 1988), occurs in southwestern Nova Scotia. The Barrington Passage Pluton is 150 kilometres southwest of Halifax. The pluton is about 60 kilometres long and 15 kilometres wide, with its long axis lying in a north-south direction. The principal study area for this thesis is the southern end of the pluton (Fig.1.1).

The Barrington Passage Pluton exhibits a foliation defined by banding of biotite-rich schlieren and prefered orientation of plagioclase and biotite. This foliation exists throughout the pluton in varying intensities. The objective of this research is to determine if the foliation results from tectonic or magmatic forces.

1.2 Regional Geology

The igneous rocks of the area intrude the host metasedimentary units of the Meguma Group, consisting of two formations, the Halifax slates and the Goldenville quartzites. The Meguma Group rocks are Cambro-Ordovician in age and they have undergone regional tectonic metamorphism to greenschist grades during the Acadian Orogeny.

Emplacement of the local plutons occurred during and after

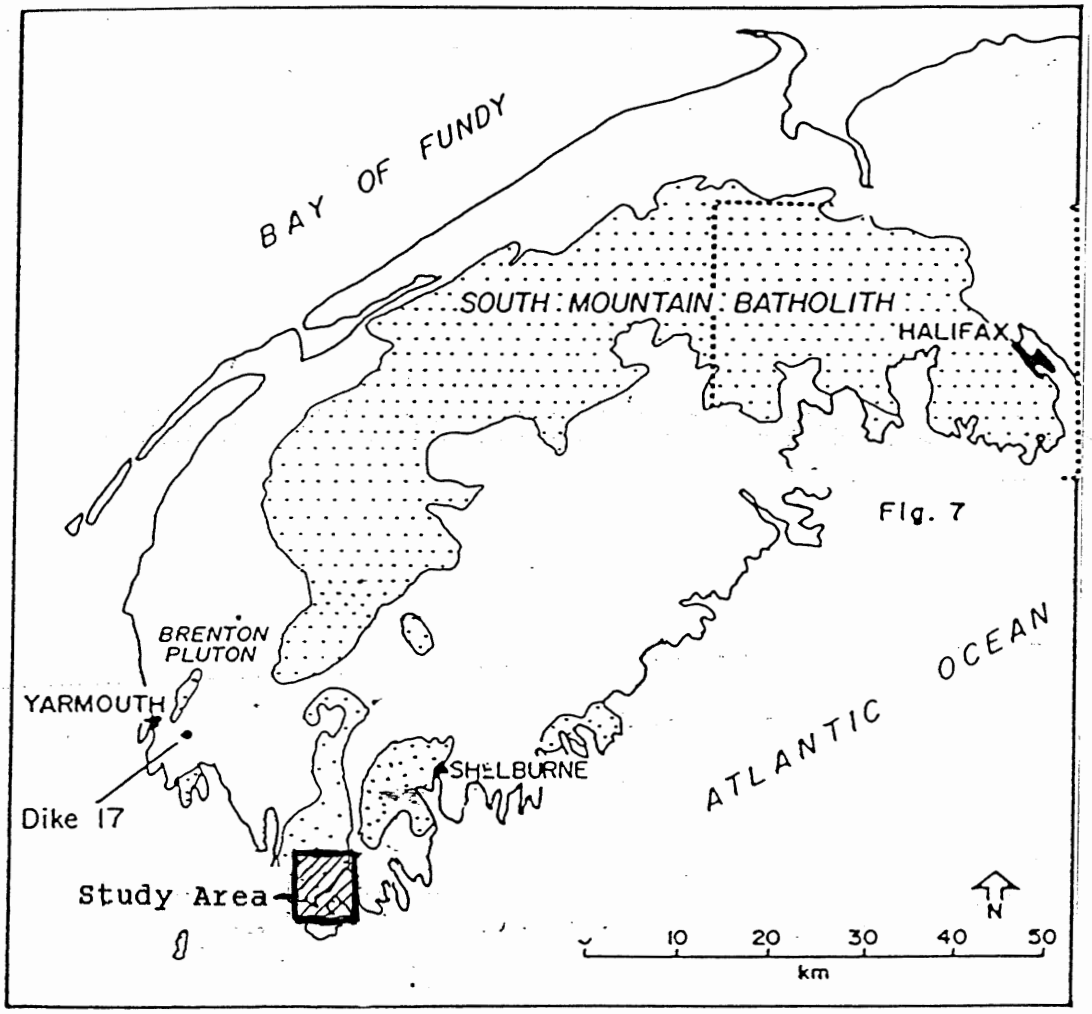

Figure 1.1 Location of the Barrington Passage Pluton study area (After Reynolds et al. 1987)

the Acadian Orogeny. Intrusions raised metamorphic grades in contact aureoles, especially around the BPP, to sillimanite - migmatite grades (Fig. 1.2). The metamorphic isograds higher than greenschist grade are concentric around the BPP (Rogers 1986).

The BPP along with the Shelburne and Port Mouton plutons, are the larger intrusions in southwestern Nova Scotia. The lithology of the igneous phases varies from biotite tonalite (BPP) to tonalite/muscovite-biotite monzogranite (Shelburne) to muscovite-biotite granodiorite/granite (Port Mouton). Smaller intrusions of the region consist of gabbronorite, hornblende-biotite tonalite and, high-K diorites (de Albuquerque 1979), that possibly relate to the larger bodies. The gabbroic body occurs in the southern part of the BPP.

The late Devonian South Mountain Batholith lies to the north of the study area. This batholith intruded around 370 Ma (Reynolds et al. 1987).

1.3 Purpose and Scope

The purpose of this thesis is to determine the origin of the foliation present in the BPP by analyzing data obtained both through field work and laboratory observations.

The geographic scope of the thesis involves the southern end of the BPP. The methodological scope involves petrographic analysis of thin sections to determine the type of foliation and its cause. The geochemical scope includes electron microprobe data and MINPET processing to determine sequence of

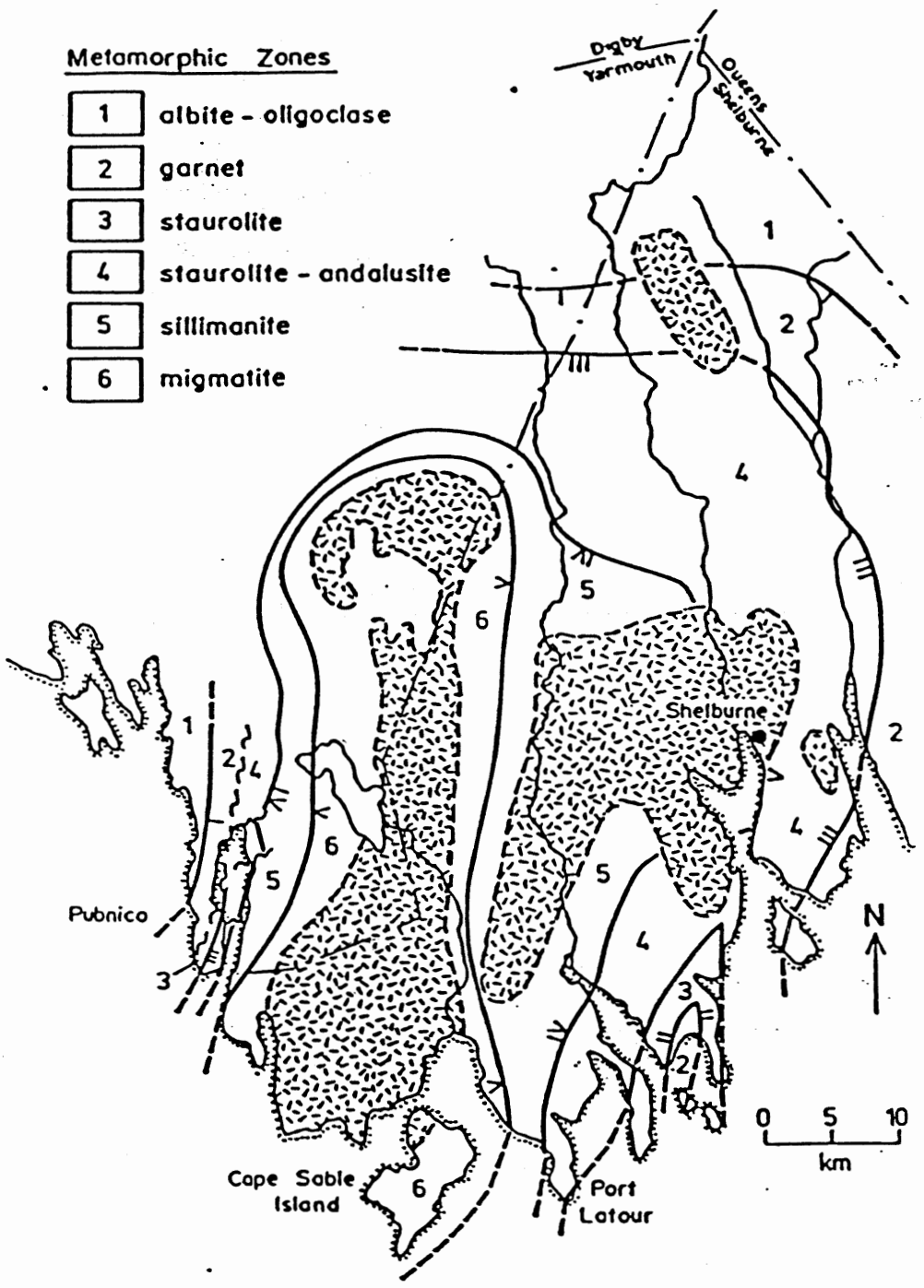

Figure 1.2 Metamorphic isograds of the study area (Rogers 1986). Note the concentric zoning of the isograds around the BPP.

crystallization and to search for zoning in the BPP. The results are categorized with the aid of the criteria developed by Paterson et al.(1988). Analysis of the criteria employed allows for differentiation between foliations of magmatic and tectonic origin. Results from this thesis will add to the understanding of the effects and timing of deformation resulting from the Acadian Orogeny.

1.4 Foliations in Granites

Development of foliations in plutonic rocks is by either tectonic or magmatic processes, or by a combination of both. Paterson et al.(1988) detail four different processes for producing foliations in plutonic rocks. The end-member cases are exclusively magmatic flowage and exclusively tectonic deformation. Between these two end-member cases are submagmatic flow in a pluton with less than the critical amount of melt, and high temperature solid state deformation.

Foliations resulting from *tectonic forces* imply that the rock experienced mechanical solid-state deformation. In this case foliations result from the recrystallizing or replacing of minerals within the pluton. These minerals orient themselves parallel to each other to minimize stress, imparting a "striped" texture to the rock. This feature is common in many tectonically deformed terranes.

Foliations resulting from tectonic forces are normally regional in character and tend to cut across different lithologies without major changes in direction. Shear zones,

however are local features with limited lateral influence (Paterson et al. 1988). During a tectonic event, dynamic stress exerted on the rocks of a region is enough to impart a foliation on them. Under these conditions, some recrystallizing of the primary minerals should occur together with the possible development of new minerals. The recrystallized minerals would orient parallel to the strain direction in the regional rocks. Therefore the foliation present in one lithology will correspond to those of neighbouring lithologies.

Foliations and banding resulting from *igneous processes* are well documented. Igneous foliations and layering are present in plutons such as the Donegal granites (Ireland)(Pitcher & Beuger 1972) and Ploumanac'h Granite (France)(Barriere 1981). These foliations originate magmatically from flow in a pluton. There are many cases in which foliations can result from flow patterns. Some features include enclaves oriented parallel to the flow with the foliation bifurcating around them, development of sedimentary type structures such as crossbedding and graded bedding (Barriere 1981), preferred orientation of primary minerals, and imbrication of elongate or tabular minerals. The orientation of the foliation may vary from location to location within the pluton. The foliations at the margins are normally parallel to the contact. Signs of solid-state deformation should be absent to ensure that the foliation is of primary (igneous) origin.

The two *intermediate cases* between magmatic and tectonic processes exhibit parts of both end-member criteria. In most

cases an overprinting of a magmatic texture by later deformation is present. Submagmatic processes involve deformation of a pluton that has a temperature less than that of the mechanical solidus, but greater than the thermodynamic solidus. The mechanical solidus is defined as the point when crystals are no longer in suspension and the magma essentially behaves as a solid, although a melt component still exists but the crystal mush behaves similar to a solid. The other case involves the deformation of the granitoid at high temperature. This type of deformation may occur soon after the pluton temperature passes below the thermodynamic solidus. Deformation and production of the foliation would, therefore, be entirely in the solid state. High temperatures make the granitoid more susceptible to stresses that can produce foliations.

Both textural and geochemical evidence is considered during evaluation of observations. Included are comparisons of the BPP observations with temperature-defined criteria of processes responsible for foliation production. These criteria outline the method of evaluating the process forming the foliation in the BPP.

1.5 Organization of Thesis

The following chapter presents field observations and structural data on foliations and other related features. Chapter 3 contains the petrographic and geochemical results of thin section and electron microprobe analyses. Chapter 4 discusses the results of the previous chapters, and makes some remarks about

the age of plutonism and deformation in the region. Chapter 5 presents a list of relevant conclusions.

Chapter 2

Field Relations

2.1 Introduction

Fig. 2.1 presents the regional geology of the study area. Field work in the area consisted of taking oriented hand samples and the measurement of foliation directions (Fig. 2.2).

The interpretation of foliation intensity is subjective. For the purposes of this thesis, the classification of foliation intensity is as follows: a weak foliation shows a limited preferred alignment of minerals and no segmentation into schlieren (Fig.2.3); a moderate foliation is recognizable and well-defined in an outcrop, and individual schlieren are laterally extensive (Fig.2.4); strong foliations have traceable, distinct schlieren bands that are equally spaced, parallel, and composed of one dominant mineral such as biotite or feldspar (Fig.2.5).

2.2 Observations of Foliations in the Barrington Passage Pluton

The studied part of the BPP covers the southern end of the pluton. There is extensive till cover and overgrowth in the study area. Most outcrops consist of road cuts, shoreline exposure, and commercial stone quarries. The colour of the tonalite ranges from whitish-grey to blue-grey, although it changes to a pinkish colour near the mafic body. The grain size of the tonalites is

medium, with little variation throughout the pluton. The foliations varied from weak (locations S-11 and HW near the centre)(Fig. 2.2), to moderate (S-16, S-13, and S-14 near mafic body and along the eastern side)(Fig.2.2), to strong at locations near the western margin. Gneissic foliations occur close to the western margin of the BPP and the country rock (locations SH 1-3 and WH [Fig. 2.2])(Fig.2.6).

The intensity of the foliation varies within single large outcrops, such as location S-10 east of Shag Harbour. At this location the foliation varies from strong to moderate within 10m. The gneissic foliations at locations SH-1 to SH-3 are very strong and strike north-south. The foliations at this location also vary within the outcrop. At location WH, near Woods Harbour, the foliation is distinct from that at other locations; here large, isolated, plagioclase phenocrysts are present between anastomosing biotite-rich schlieren.

At locations S-12 eastward to S-14, the foliations consistently align NNE-SSW. There is evidence of considerable alteration of the tonalite in this area, from its usual bluish colour to a tan or faint pink colour. This alteration could result from the intrusion of the mafic body which outcrops along the road between location S-16 and S-14 (Fig.2.1).

Eastward, at the old stone quarry (Fig. 2.1), the foliation strike changes by 90° to a WSW-ENE orientation. The longest continuous lateral extent of outcrop is at this location.

The foliations at locations S-1 to S-9 and S-18 are all

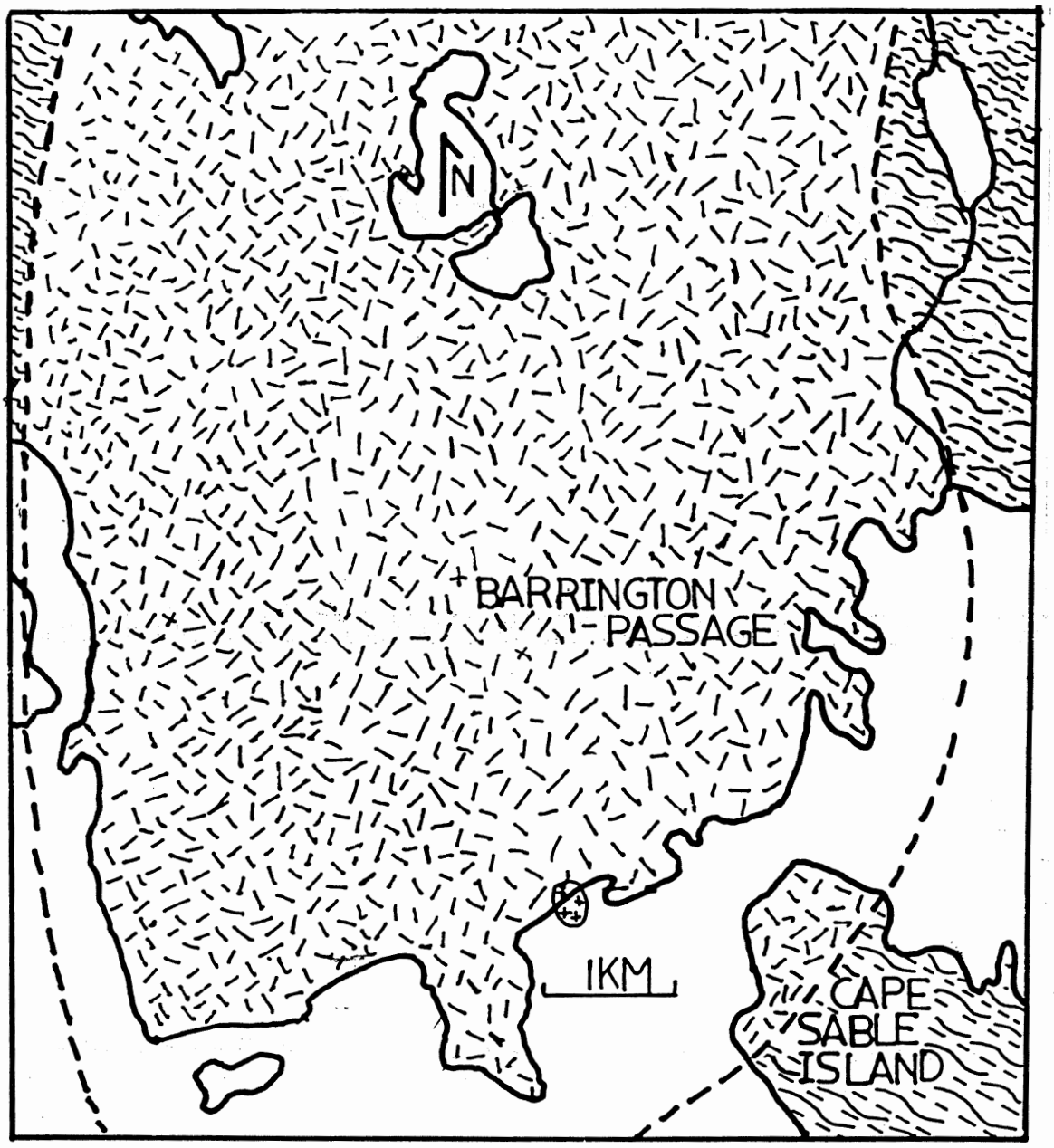

Barrington Passage Pluton (tonalite)

Meguma Group (Goldenville Formation/ Quartzites)

Norite

Figure 2.1 Lithology of the study area (Base Map after Rogers 1986)

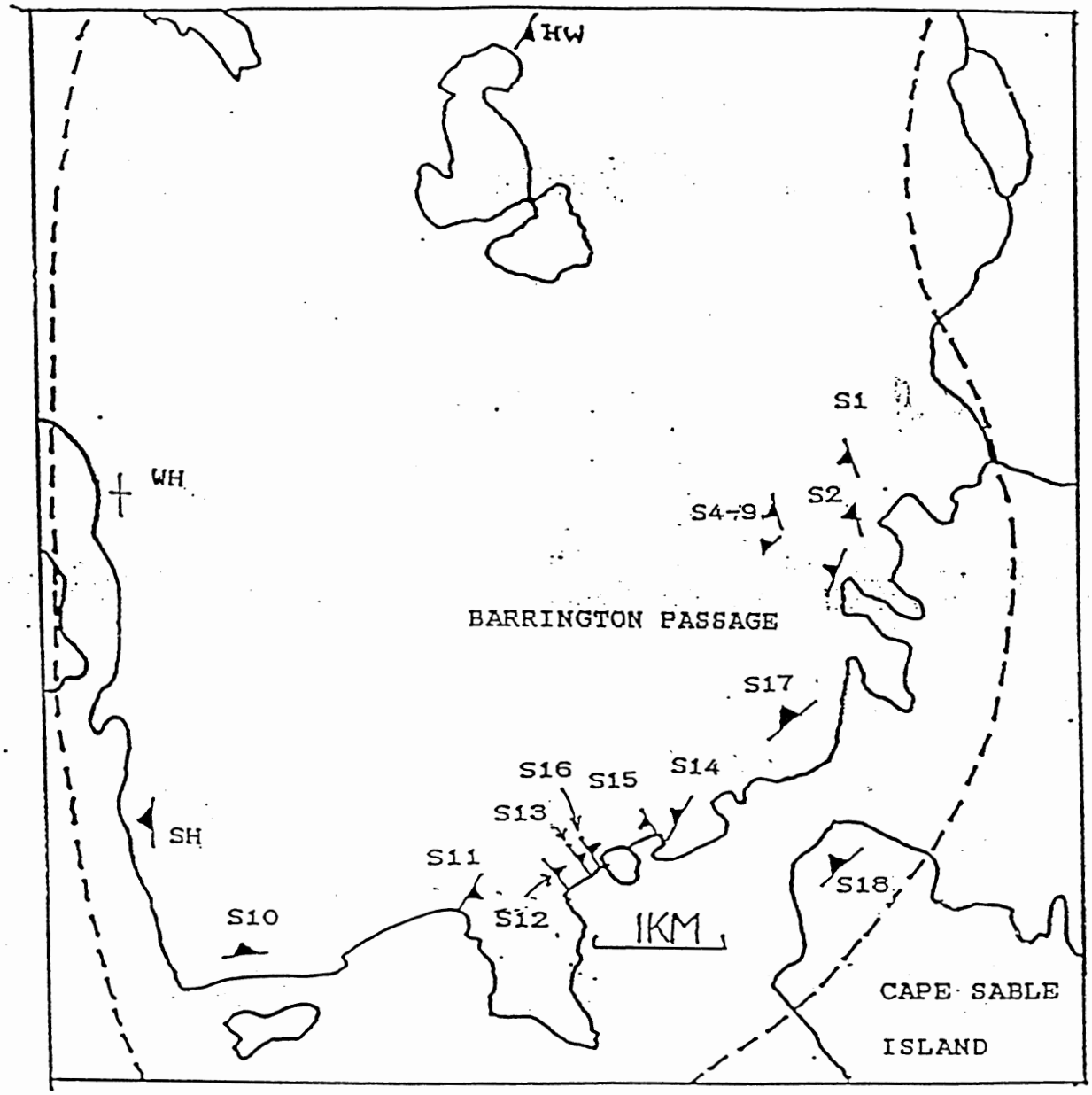

Figure 2.2 Sample locations and foliation measurements of the study area outcrops. (Base Map after Rogers 1986)

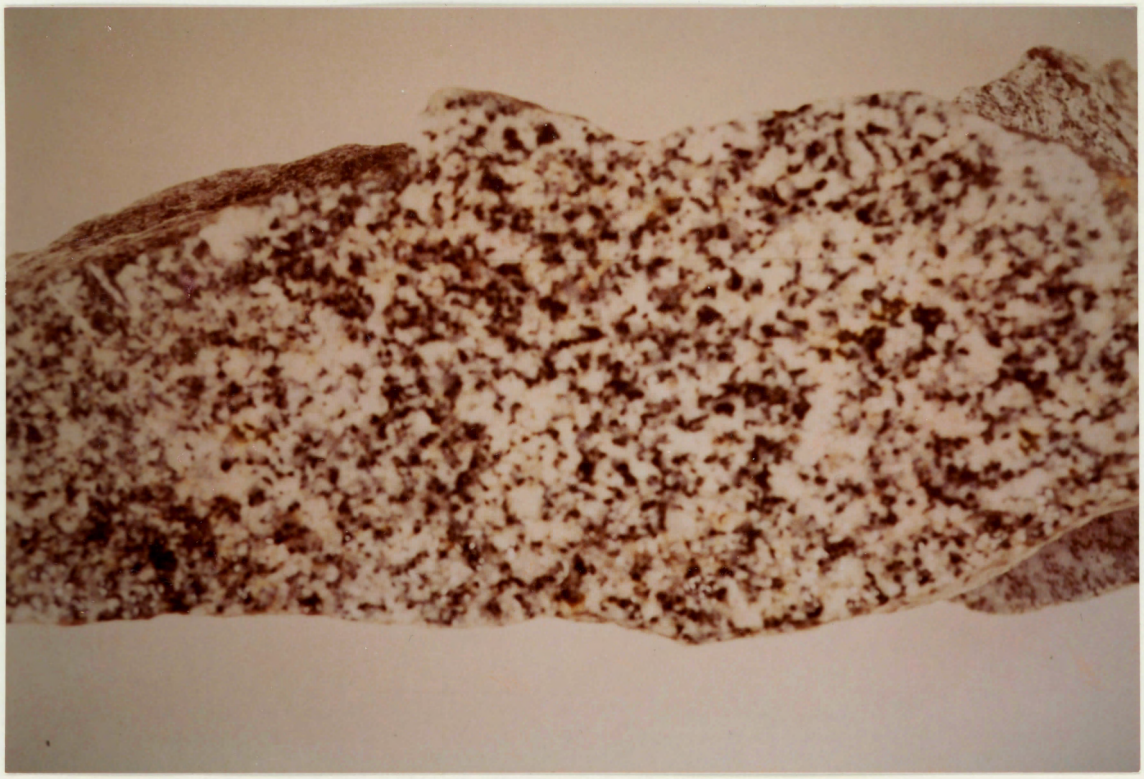

Figure 2.3 Weak foliation in hand sample from location HW. Note the lack of any defined foliation direction. Field of view is 28 cm across.

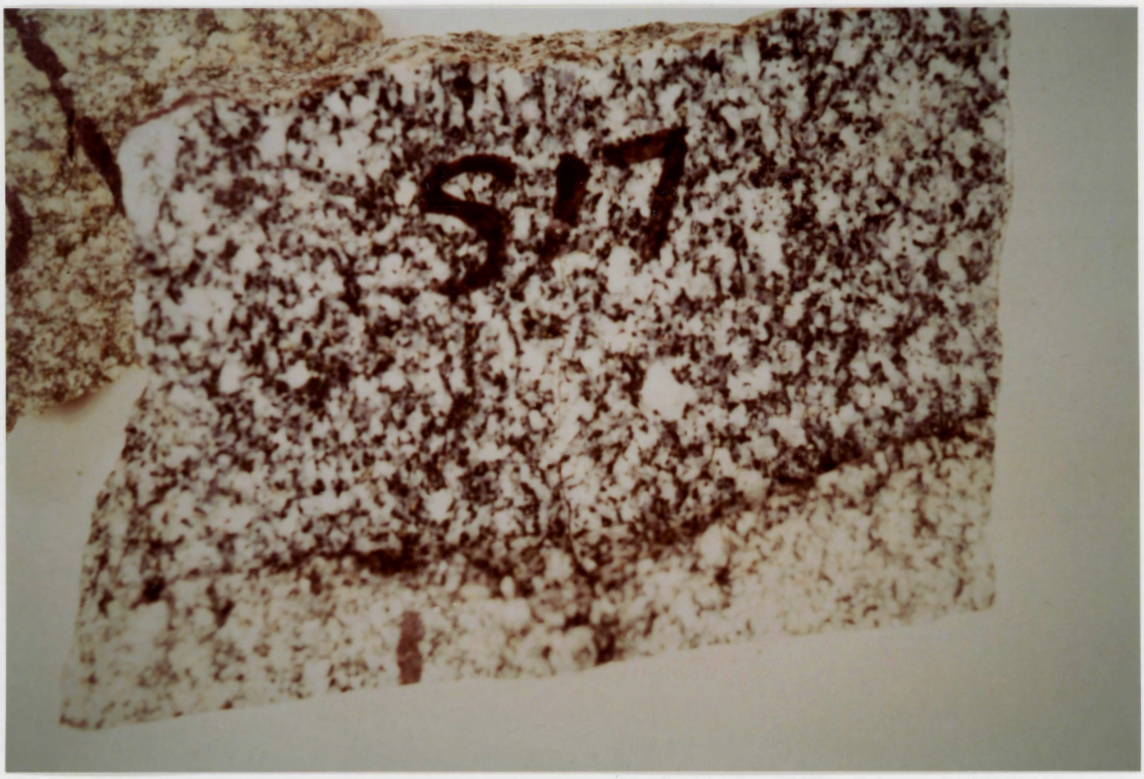

Figure 2.4 Moderate foliation in hand sample from location S17. A slight preferred orientation is visible, orienting from top to bottom of the figure. Field of view is 18cm across.

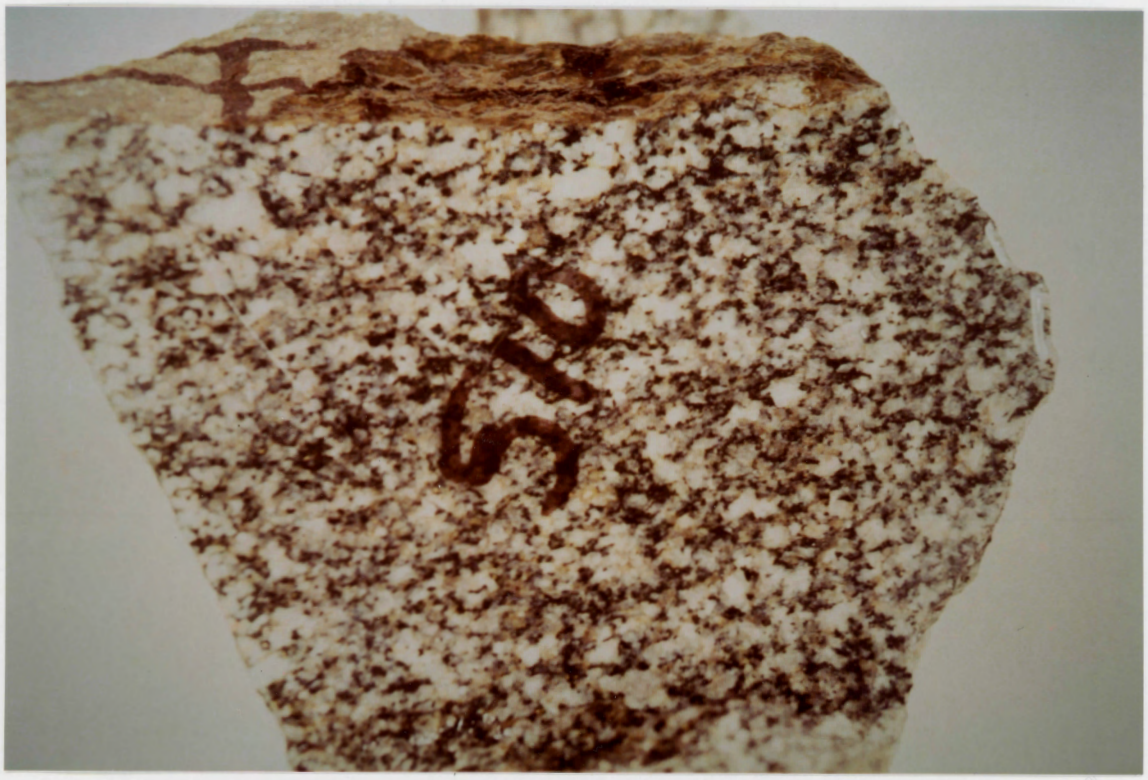

Figure 2.5 Strong foliation in hand sample from location S10. This sample displays some schlieren layering and strong preferred orientation. Field of view is 18cm across.

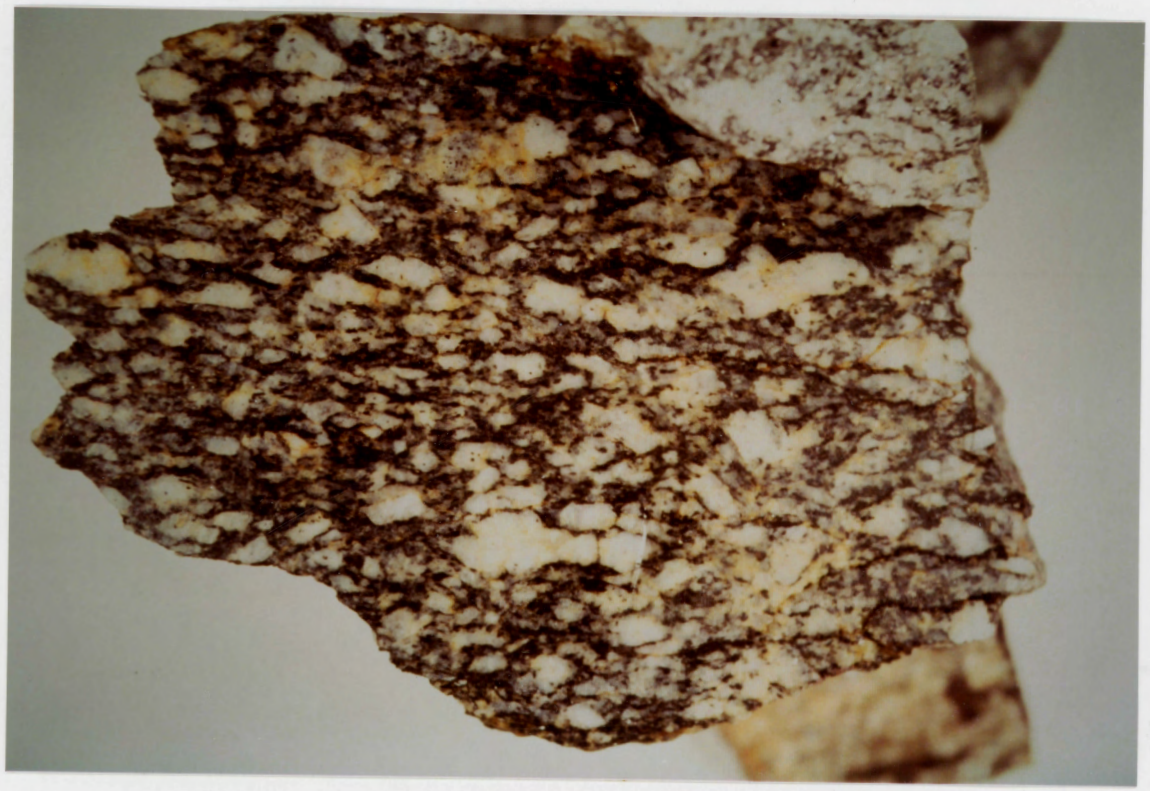

Figure 2.6 Gneissic foliation in hand sample from location WH. Note the anastomosing character of the biotite layers around the plagioclase crystals. Field of view is 18cm across.

subparallel to the contact of the BPP with the country rocks. Foliations measured in the new stone quarry (Fig.2.1)(samples S-4 to S-9) show only a small variation in attitude within the extent of the outcrop. The dips in this area are also shallower than the dips to the west.

In summary, the foliations vary in intensity and orientation within this pluton. Not all of the foliations are consistent with the regional tectonic trends in the country rocks. Foliations close to the contacts are parallel or sub-parallel to the trend of the contact; foliations toward the interior are random.

2.3 The Mafic Body and Influence on the BPP

Rogers (1986) classified the mafic body at the southern end of the BPP as a diabase, and de Albuquerque (1979) classified it as a norite. A more precise classification of the body follows in the next chapter. Most of the outcrop lies offshore in Murray Cove, however the outcrops near Atwoods Brook are roadcuts and shoreline. The mafic body also occurs on the islands within Murray Cove. It is a greenish-black rock with some surficial signs of weathering, especially in the shore outcrop. The body is massive, with no signs of deformation or of a foliation.

According to de Albuequerque (1979) the BPP completely encloses the mafic body. Analysis of aeromagnetic maps of the area indicate the body is roughly circular and approximately 500m in diameter and completely enclosed within the BPP.

2.4 Enclaves and their Relation to the Foliation

Enclaves in the BPP include distinct metasedimentary xenoliths of the country rocks, and other samples of uncertain origin. These latter enclaves could be metasedimentary xenoliths at advanced stages of incorporation into the magma, or they could be microgranitoids derived directly from the magma. Most enclaves have a subrounded shape and align parallel to the foliation (Fig.2.7). The only exception is a tabular enclave at S-10 which has a pronounced bend. In some cases the enclaves appear to have "tails" (Fig. 2.8). The tails are small elongate appendages tapering out from the parent enclave. Enclaves with tails occur in the eastern parts of the study area,and they all point in a general westward direction. Some of the enclaves appear elongated and stretched to the point of resembling schlieren (Fig. 2.9). The foliation never cuts across the enclaves but rather bends and bifurcates around them. Elongate enclaves align parallel to the foliation. In one case, at location S-10, an enclave bends plastically within the tonalite (Fig.2.10). Other enclaves observed bend around larger enclaves (Fig.2.11).

2.5 Shear Zones and Faults within the BPP

One fault within the BPP is present at location HW, and is about thirty centimetres wide containing fault gouge. Deformation of the tonalite laterally from this fault is minimal, with all effects disappearing within one metre of the fault. There is apparent deformation involved with samples along the

Figure 2.7 Enclaves within the foliations. Note that the foliation bends around the enclave and does not pass through it. This sample is from rubble at the new stone quarry (Fig.2.1).

Figure 2.8 Enclave with a "tail" at Location S17. This enclaves is one of several visible in the old stone quarry. Most of the enclaves possess these tails and all the tails point in the same direction, suggesting that deformation was homgeneous and is not the result of preferred deformation of one type of enclave.

Figure 2.9 Shortened and deformed enclaves at location S5. These enclaves from the new stone quarry are different in shape from most other enclaves, suggesting that they may have been preferentially deformed, or are older and more deformed enclaves.

Figure 2.10 The sedimentary xenolith at location S10. This xenolith has a pronounced bend of unknown origin. The foliation follows the bend in this xenolith.

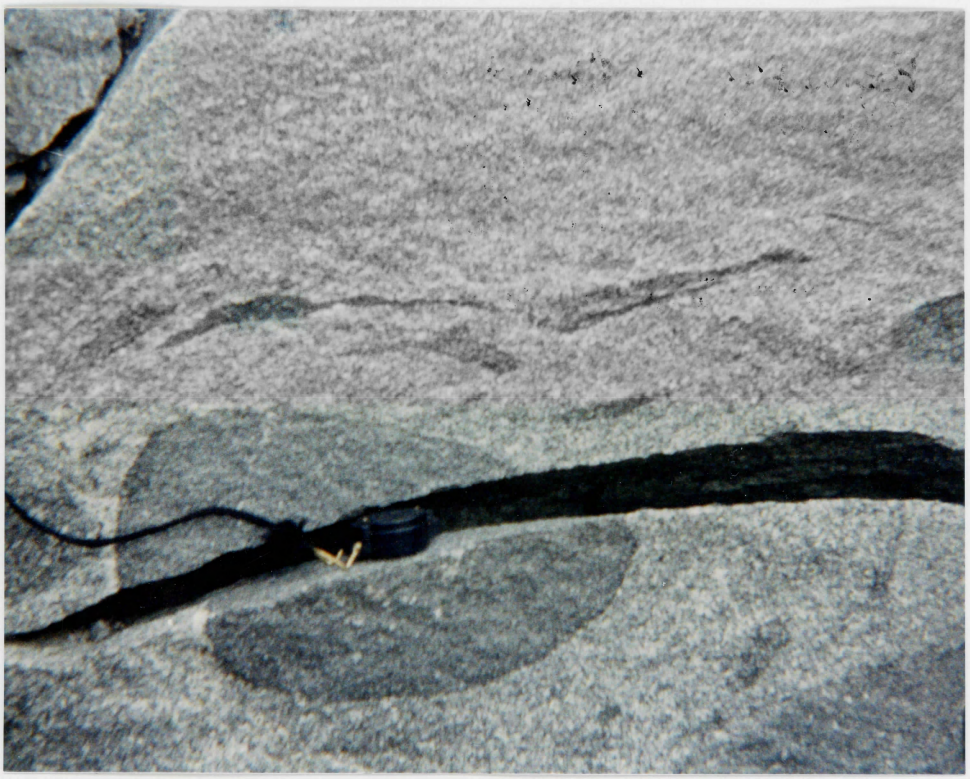

Figure 2.11 Smaller enclaves bending around larger enclaves at location S17. This implies that enclaves are bent by the same forces that produced the foliation.

western margin of the BPP, that may show evidence of ductile deformation like S-C foliations and deformed primary schlieren.

2.6 Contact Relationships of the Country Rock and the BPP

Contact studies consist of one Meguma outcrop on Cape Sable Island consisting of migmatized country rock. This outcrop location is about 500m from the inferred contact. According to Rogers (1986), the contact consists of migmatized country rock forming a zone 500-1000m wide around the pluton.

2.7 Minor Intrusions

There are many smaller intrusions observed in the BPP. The Shelburne dyke cuts the BPP to the north of the study area. There are many pegmatites in the BPP, consisting of K-feldspar and quartz as the principal components. Most of the pegmatites cut the plane of the foliation at high angles, with no observed foliation or deformation present in the pegmatites. Other veins appear to cut the BPP randomly. All crosscut the BPP and are, therefore, younger.

2.8 Conclusions

The foliation within the BPP is heterogeneous both in attitude and intensity. Foliations bend and curve around enclaves instead of passing through them. Some enclaves stretch and deform while others show no apparent signs of deformation. Elongate enclaves align parallel to the foliation. Those foliations nearest the margins align parallel to the contact. Schleiren layering is common throughout most of the pluton.

The tonalite of the BPP near the mafic body appears altered.

This could be the result of contact effects from the intrusion of the mafic body into the BPP. Foliations to the west and east of the body align in a north-south direction.

Observed faults and shear zones have only a local effect on the pluton and could have no influence on the foliations of the whole pluton.

The foliations, while parallel to the contacts, do not appear to be continous with the structural trend of the Meguma Group rocks.

Chapter 3

Petrography and Geochemistry

3.1 Introduction

Biotite tonalite comprises most of the rocks of the study area. For the purposes of this paper the rocks of the study area separate into four categories: biotite tonalite, a mafic body, the enclaves within the BPP, and pegmatites of the area. Each of the four groups differ from the other significantly, but there is little variation within each of the groups. This chapter discusses the results of petrographic and geochemical analyses of the representative samples from each group.

3.2 Petrography

3.2.1 BPP Tonalite

The tonalite of the BPP are whitish-grey to blue-grey in colour, and medium-grained and hypidiomorphic in texture. The average modal composition of the rock is: plagioclase 50%, biotite 25%, quartz 20%, alkali feldspar <5%. The classification is a tonalite (Streckeisen, 1974). Other minerals are, hornblende, apatite, titanite, epidote, muscovite, chlorite, rutile, sericite, and opaque minerals (magnetite and sulphides).

Plagioclase, combined with biotite, defines the foliation. Plagioclase occurs as fine- to medium-grained, elongate, subhedral crystals. Some crystals exhibit compositional zoning (Fig. 3.1) and most show polysynthetic twinning. Slight

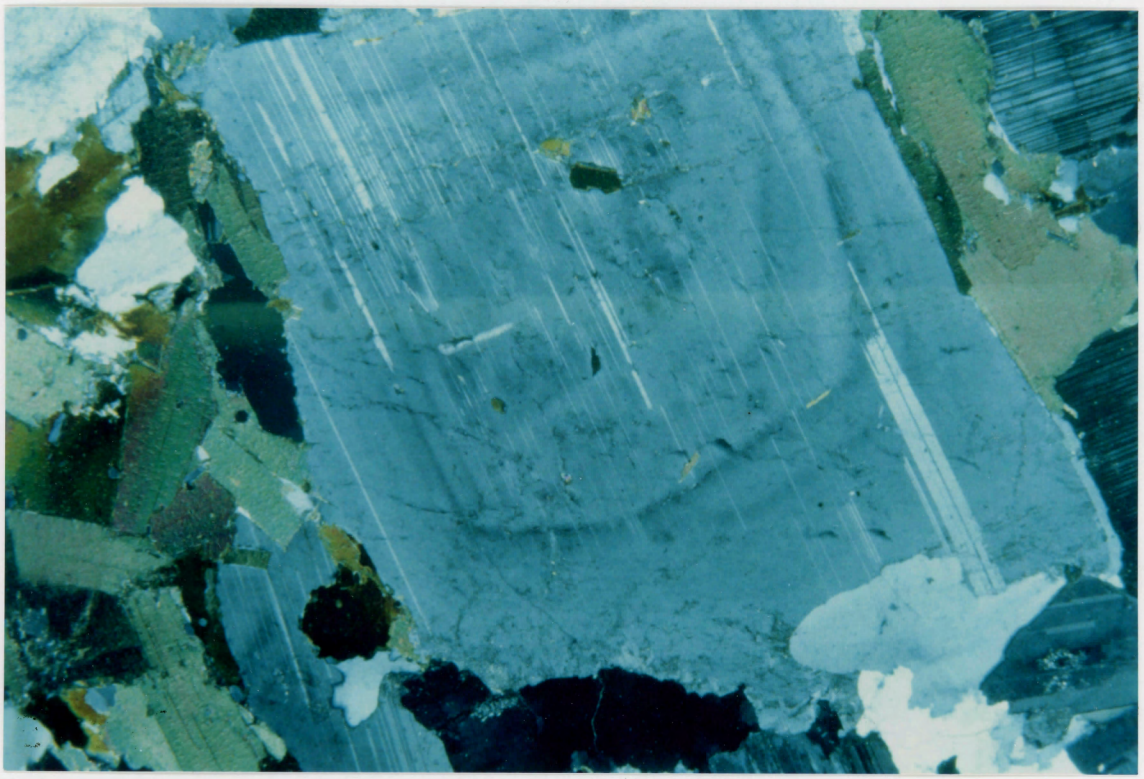

Figure 3.1 Igneous concentric zoning of plagioclase at location S5. This zoning occurs with the progressive overgrowth of plagioclase of differing compositions within the magma. Scale of the photo is 4 mm across.

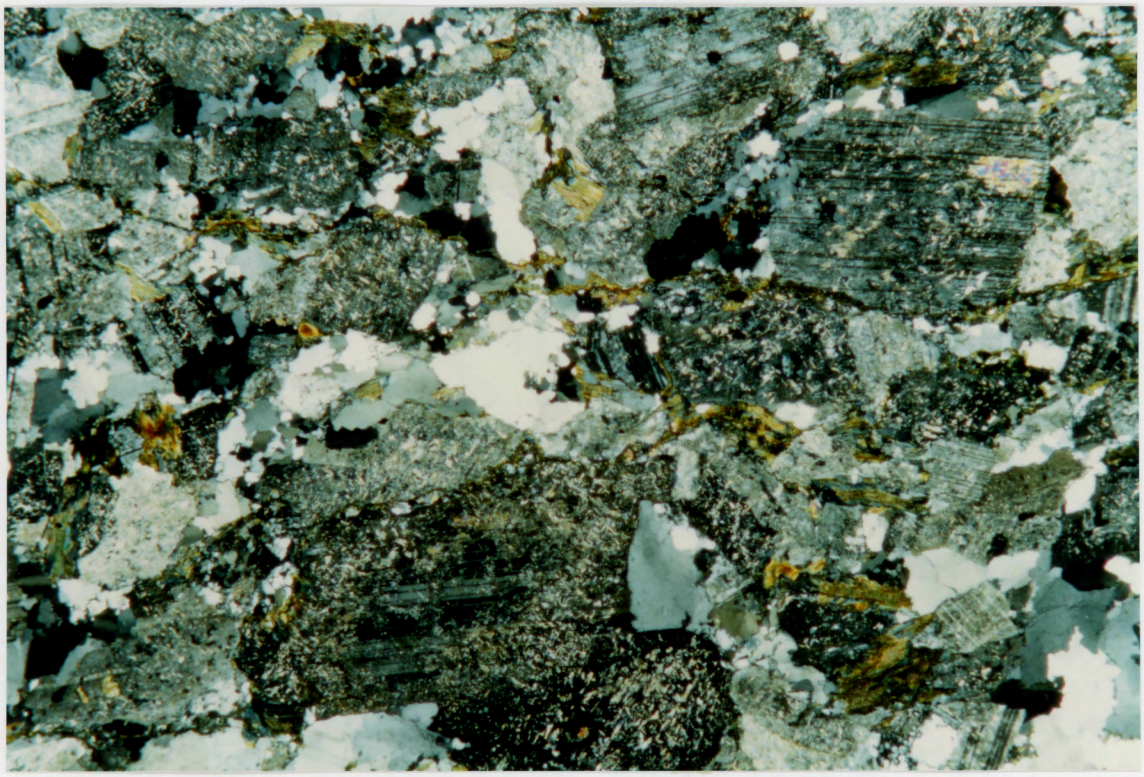

Figure 3.2 Sample S12 showing the strong alteration of the plagioclase close to the mafic body. The nearly complete replacement of plagioclase by sericite characterizes this alteration. Scale of the photo is 20 mm across.

alteration to sericite and epidote occurs in most plagioclase crystals, but strong alteration is present in the samples close to the norite (Fig. 3.2). Fractured and rounded plagioclase occurs in the western margin samples along with plastically deformed crystals defined by bent polysynthetic twins (Fig. 3.3). Imbricated plagioclase occurs in some samples, with the plagioclase oriented in a different direction from biotite (Fig. 3.4)

Biotite is anhedral to subhedral in shape. It is the mineral most likely to define the foliation on account of its platy habit (Fig. 3.5). Biotite is altered slightly to chlorite and muscovite in places (WH and SH). Some recrystallization of biotite into fine-grained aggregates is also evident (S13, S16, and S15). In samples SH and WH the biotite expelled opaque inclusions (Fig. 3.6).

Quartz occurs as fine- to medium-grained anhedral aggregates or medium-grained anhedral crystals with mosaic or undulose extinction (Fig. 3.7). Larger crystals do not possess a preferred orientation. Quartz also occurs as fine-grained aggregates throughout the BPP, aligned parallel to the foliation.

Alkali feldspar occurs as microcline. Throughout the BPP, K-feldspar crystals occur as rare, unaltered, subhedral grains that are smaller than plagioclase crystals.

Epidote is present as fine-grained masses, or as large euhedral crystals among veins. A study by Zen and Hammarstrom (1984) has shown epidote to be a common primary mineral in

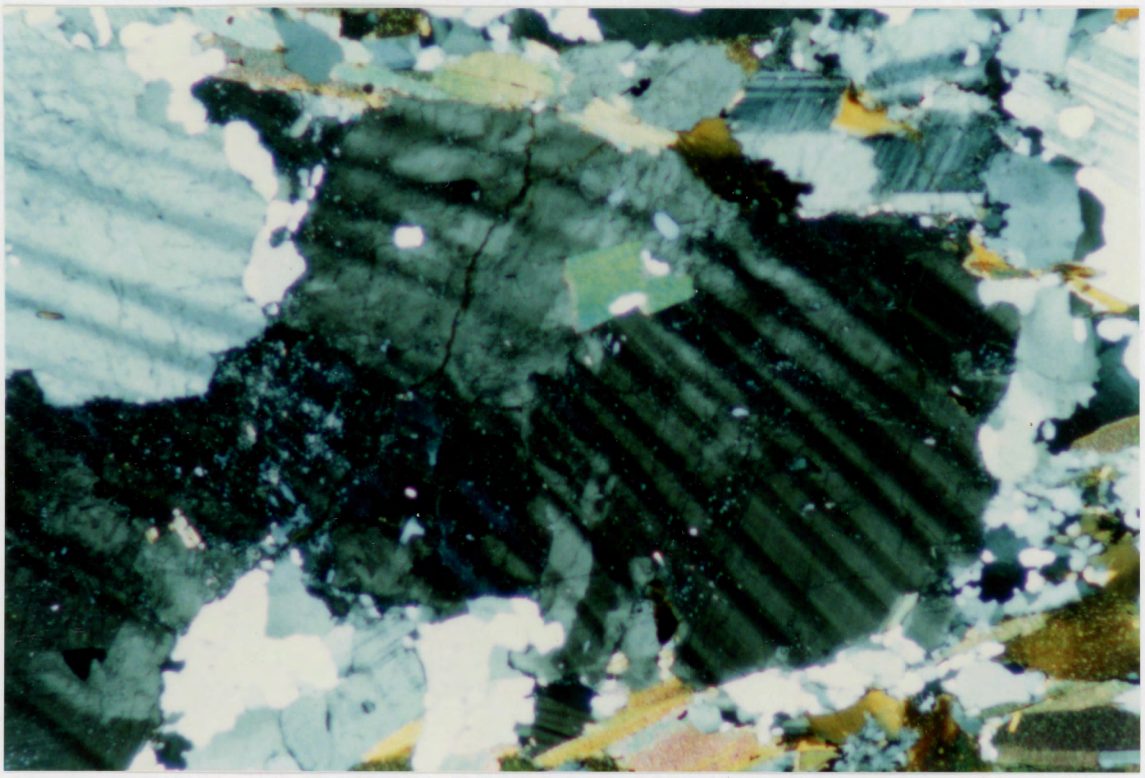

Figure 3.3 Sample WH, in which bending of the polysynthetic twin lamellae, without fracturing, implies plastic deformation. This sample is from location WH. The of the photo is 2mm across.

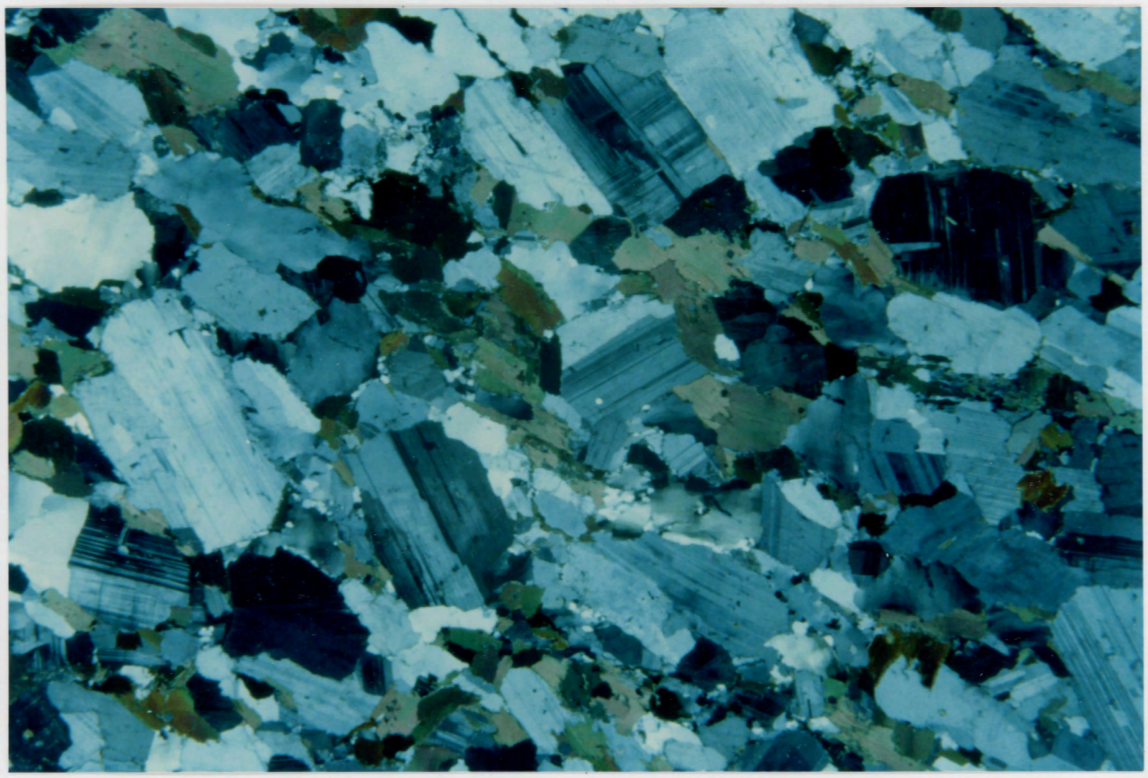

Figure 3.4 Imbrication of plagioclase within a flow may explain the preferred orientation of plagioclase at an angle to the dominant foliation defined primarily by biotite in this case. The sample is from location S1. The scale of this photo is 20 mm across.

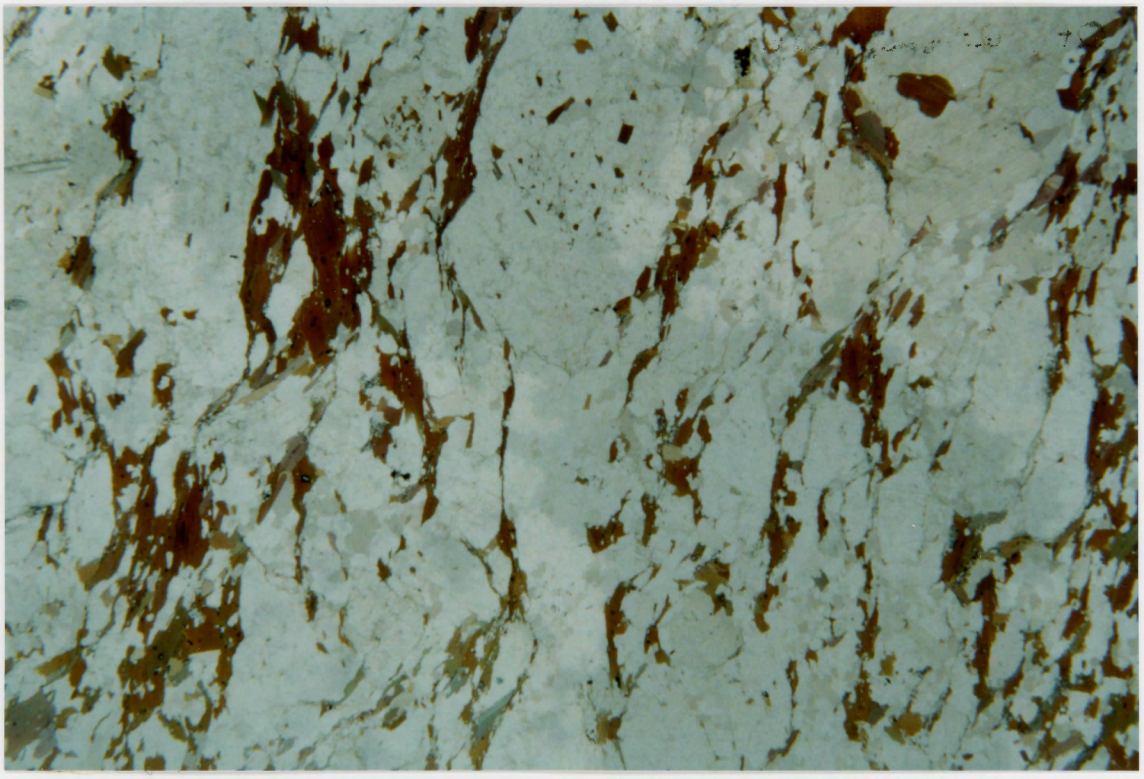

Figure 3.5 Biotite is often the best indicator of the actual foliation orientation, as shown by the alignment observed at location WH. The scale of the photo is 20 mm across.

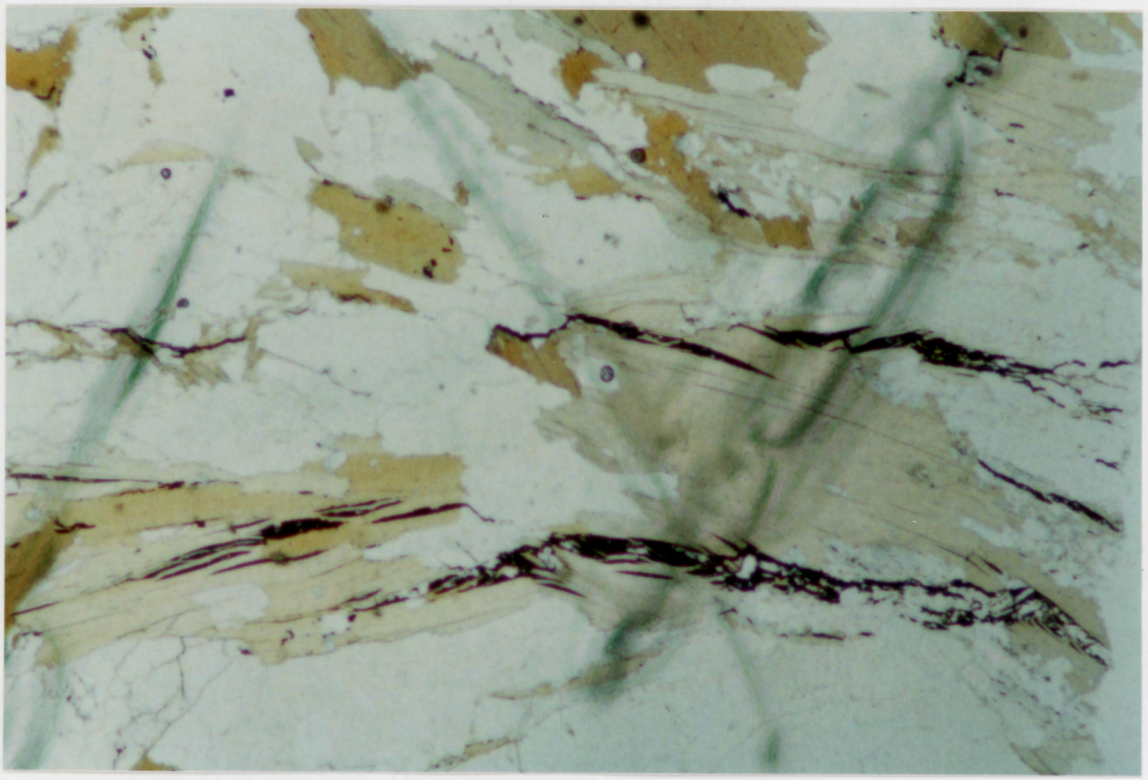

Figure 3.6 Segregation of opaque minerals into cleavage traces is common in biotite from location WH. Opaque minerals occur at the margins of biotite or parallel to the cleavage in the biotite. The scale of the photo is 3 mm across.

plutons of tonalitic to granodioritic compositions. Epidote occurs as a late phase, forming from a hornblende-liquid reaction (Fig. 3.8). Laboratory experiments imply that it forms under pressure at mid-crustal depths or deeper.

Apatite is a common mineral in the tonalite, occurring as very fine-grained, isolated, equant, subhedral crystals.

Titanite is another common mineral. Titanite is very fine-grained, often occurring with biotite and appearing as aggregates or isolated, subhedral to euhedral grains.

Rutile is a common accessory mineral in biotite. It occurs as acicular inclusions in biotite crystals. These elongate inclusions sometimes have three different orientations within a single grain that all meet at an angle of 60°.

Muscovite occurs as fine euhedral grains within biotite aggregates, as inclusions in biotite, or as fine-grained anhedral to subhedral crystals among biotite.

Sericite is a common secondary mineral produced from the alteration of plagioclase and biotite. It occurs as fine-grained masses in the centres and margins of altered plagioclase crystals and along the margin of biotite. At locations around the mafic body, sericite almost completely replaces plagioclase (Fig. 3.2).

Chlorite is a common secondary mineral produced from the alteration of biotite and appears as fine grained masses.

The grain size of the BPP is uniform throughout the study area except for locations WH and SH 1-3 where the grain size is coarser. Most alteration of the tonalite is generally weak,

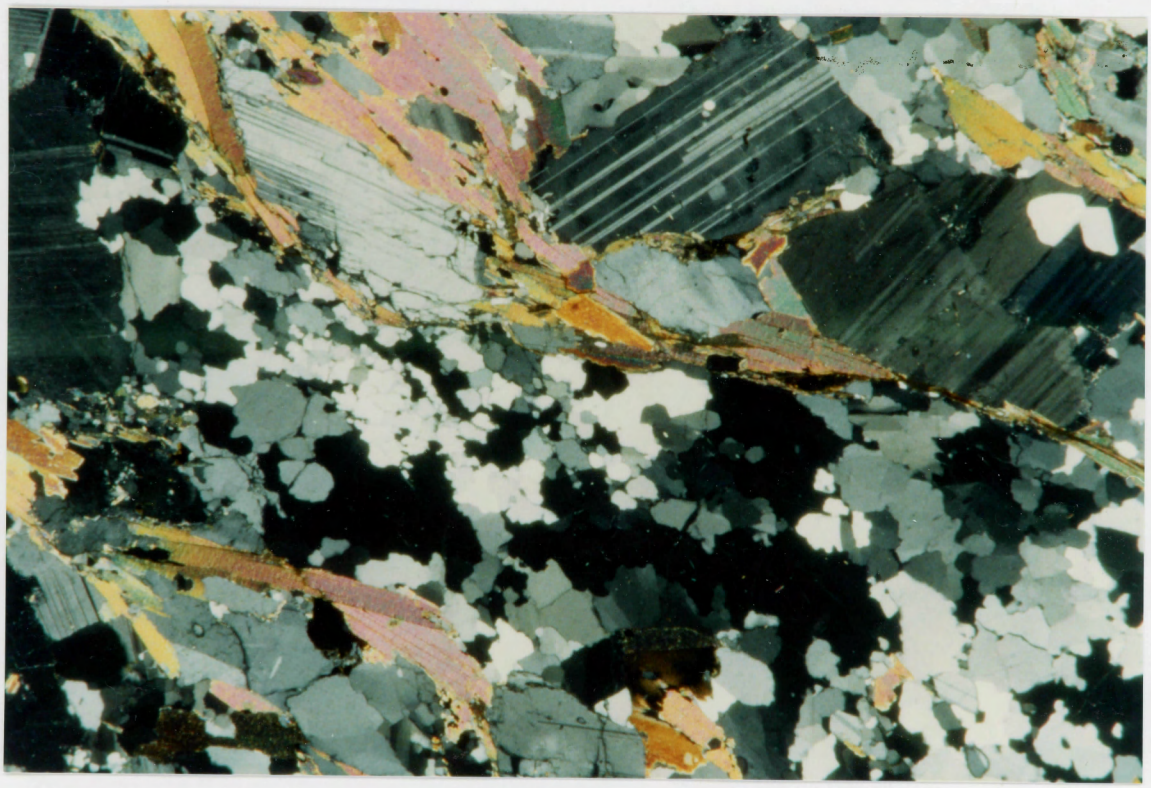

Figure 3.7 Quartz occurs mainly as aggregates consisting of fine-grained quartz oriented parallel to the foliation, such as the aggregates shown, from location WH. The scale of the photo is 4 mm across.

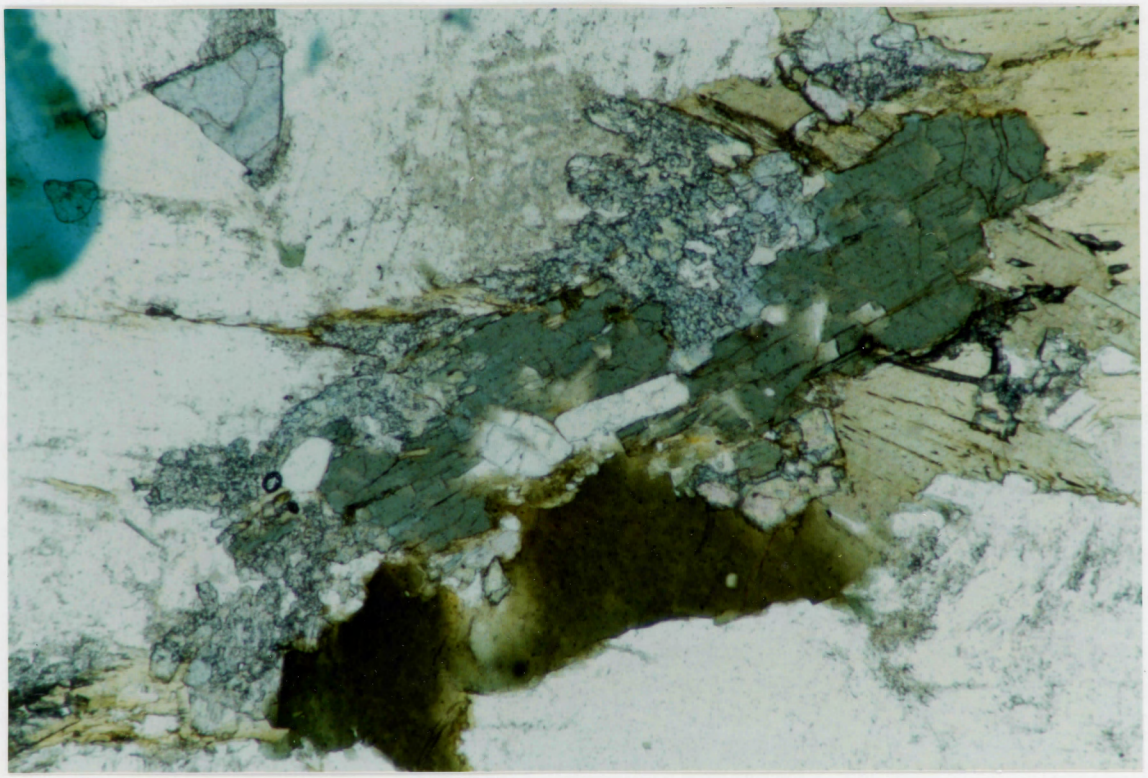

Figure 3.8 Hornblende is a rare mineral within the tonalitic rocks. It is usually found as altered xenocrysts, such as the one shown, from location S1. Hornblende from the BPP tonalite alters to epidote. The scale of the photo is 2 mm across.

except for the strong alteration at the locations closest to the mafic body. This alteration may be hydrothermal, resulting from the intrusion of the mafic body. Preferred orientation of biotite and plagioclase characterizes the BPP foliation (Fig. 3.9). Plagioclase alignment is common, but not to the degree of biotite. The foliation appears generally to be strongest at the locations nearest the contacts.

3.2.2 The Mafic Body

The mafic body at Murray Cove consists primarily of orthopyroxene, clinopyroxene, and plagioclase. The average modal composition of the mafic body is: plagioclase 40%, clinopyroxene 30%, orthopyroxene 25%, opaques <5%. The mafic body is classified as a gabbronorite (Streckeisen, 1984), but is simply referred to as a norite for the purposes of this paper.

The norite grain size and compositions are variable. Variations are slight in modal composition, ranging from a melagabbronorite to a leucogabbronorite. The norite grain size is medium-grained, with numerous coarse-grained gabbroic dykelets crosscutting the main body. These small gabbroic pegmatites are of norite composition. Most dykelets are less than 5 cm in width and have indistinct boundary contacts with the norite. Granitic pegmatite dykes (composed of K-feldspar,plagioclase, quartz, muscovite and magnetite) up to 40 cm in width cut the norite body.

The norite is massive and has no foliation or any other internal structure.

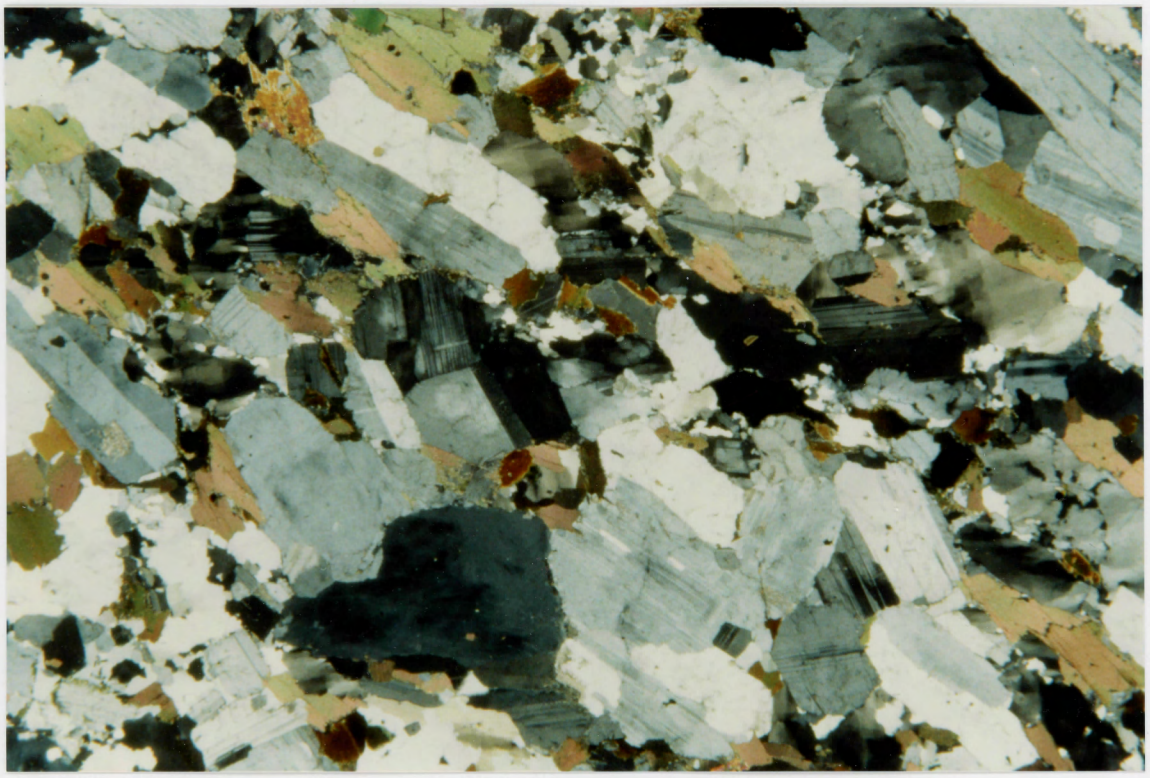

Figure 3.9 Throughout most of the BPP, primary minerals define the foliation, with biotite and plagioclase being the most strongly oriented minerals, as shown in this sample from location S1. The scale of the photo is 20 mm across.

3.2.3 Enclaves

Most of the enclaves are massive and fine-grained. Modal compositions of the enclaves are: plagioclase 35%, biotite 50%, and quartz 15%, with one enclave enclave at S2 containing 20% modal hornblende. Some enclaves have a preferred orientation of biotite while others do not. The preferred alignment observed meets the host rock foliation at an angle. The enclave at S-10 has distinct internal bedding and is concluded to be of metasedimentary origin. (Fig 2.10). Most of the darker enclaves contain large plagioclase phenocrysts that span the boundary between enclave and tonalite.

3.2.4 Pegmatites

Several pegmatite dykes occur within the BPP with compositions: K-feldspar 40%, quartz 25%, plagioclase 20%, muscovite/biotite 10%, and opaques 5%. The crystals of each mineral are subhedral to euhedral in shape. The grainsize of these dykes is coarse, and the size of the dykes themselves is greater than 25cm in width. These pegmatites exhibit no signs of deformation except for a slight undulose extinction or polygonization of quartz.

3.3 Geochemistry

The results of the microprobe analyses and MINPET data plots suggest that the pluton is homogeneous in composition. It is thought that plutons probably crystallize from the margins inward, by a process of convective fractional crystallization. If so, the foliations should be parallel to the pluton walls.

Because of fractional crystallization, a gradation from phlogopitic to siderophyllitic biotite should be observed. This involves an exchange of Fe for Mg along with an exchange of Al for Mg and Si. Plagioclase will exhibit a continuum from calcic plagioclase to more sodic plagioclase. In general, there should be a gradational chemical change in the samples from the margins of the pluton inward, or from the core to the rim within individual crystals. Compositions of both biotite and plagioclase exhibit no such progression (Fig. 3.10).

3.4 Significance and Conclusions

Biotite, plagioclase and quartz are the principal minerals comprising the BPP tonalite. Biotite and plagioclase define the foliation observed in the BPP. Biotite shows the greatest alignment with the foliation. Plagioclase aligns subparallel to parallel to this foliation. Both minerals have subhedral to euhedral grain shapes and are primary (igneous) minerals. Some recrystallization of biotite and plagioclase occurs in samples from the western margin and norite margins, with plagioclase becoming rounded or fractured and biotite altering to chlorite. Plagioclase alters to sericite, with sericite almost completely replacing the plagioclase at locations nearest the norite body. Otherwise, plagioclase alteration is minimal. Plagioclase locally displays an imbricated texture. Quartz occurs as either anhedral, deformed grains, or as fine-grained aggregates.

Clinopyroxene, orthopyroxene, and plagioclase comprise the norite and all the minerals are primary and igneous in origin.

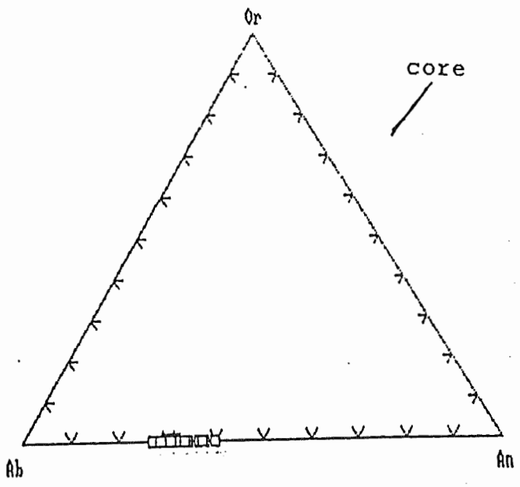

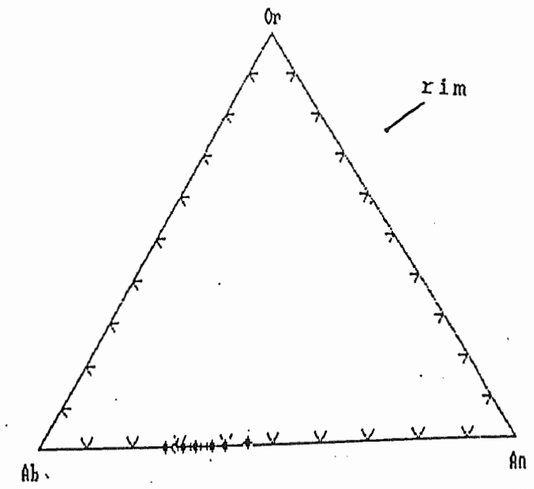

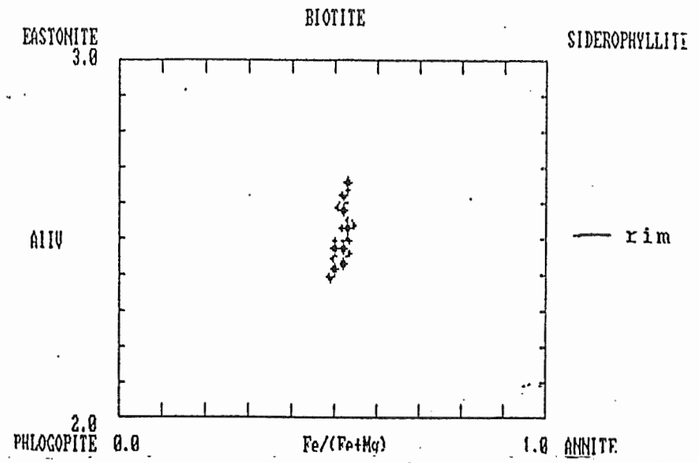

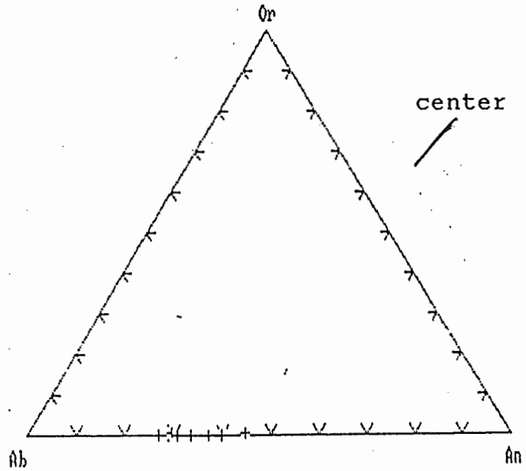

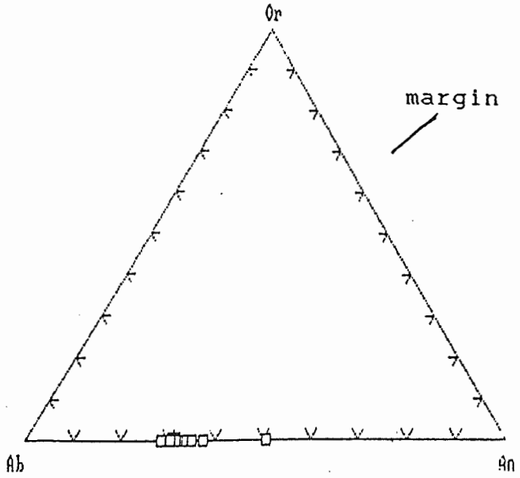

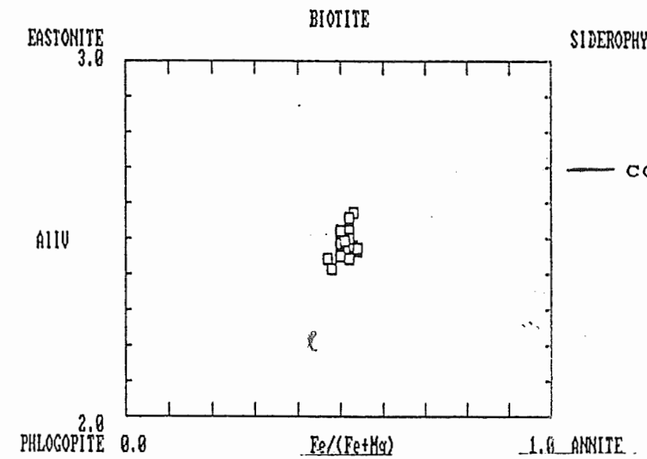

Figure 3.10 Plots of electron microprobe data by the MINPET program show that there is no consistent chemical change trend between samples from the margins and centre of the pluton, or from the core to the rim in individual minerals.

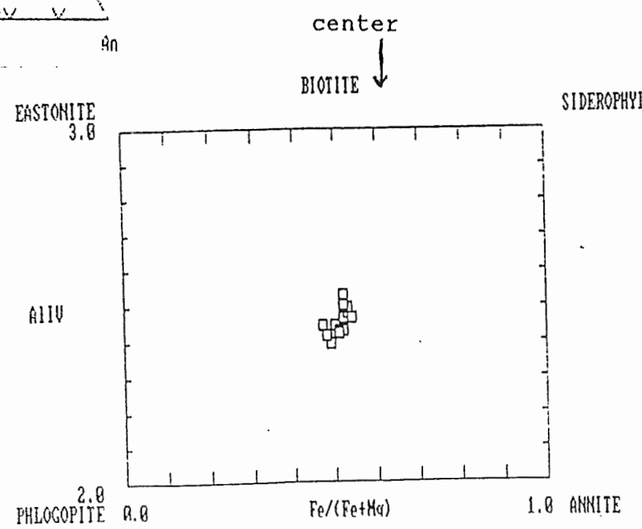

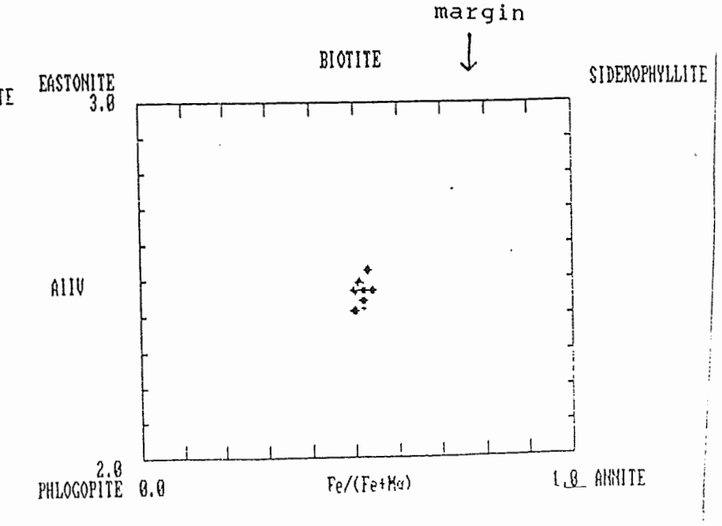

There is no microstructural evidence of deformation in the norite or any preferred orientation of primary minerals in the norite.

Biotite, plagioclase, quartz and hornblende compose the enclave mineralogy. Some enclaves possess an internal preferred orientation of biotite while others do not. There is some evidence of polygonized quartz within the enclaves.

K-feldspar, quartz, plagioclase, and muscovite comprise pegmatites and other minor intrusions within the BPP. There is only a slight undulose extinction of quartz observed within the pegmatite samples.

Geochemical analyses of the samples show that the pluton has a homogeneous compostion, with no evidence to suggest fractional crystallization inward from the margins.

Chapter 4

Discussion

4.1 Introduction

This chapter evaluates the significance of the observations, presented in the previous chapters, according to the criteria proposed by Paterson et al. (1988). A single type of observation can rarely define the origin of foliation. Instead each criterion is part of a group of criteria and together they help to define the processes that could produce a foliation in a granitoid rock. These processes are part of a continuum between entirely magmatic and entirely tectonic processes as the end-members (Paterson et al. 1988). A foliation may be the result of one process or of a combination of the following processes:

1) Magmatic
2) Sub-magmatic
3) High-temperature solid state deformation
4) Low- to moderate-temperature solid state deformation

Figure 4.1 shows the pressure-temperature conditions of the four domains. To analyse the data from the BPP, the pluton is broken up into four sections: the western margin of the BPP, the south central part, locations surrounding the norite body, and the eastern margin (Fig. 4.2)

4.2 Methods of Producing Foliations in Granitoid Rocks

Table 4.1 lists the criteria involved in the production of

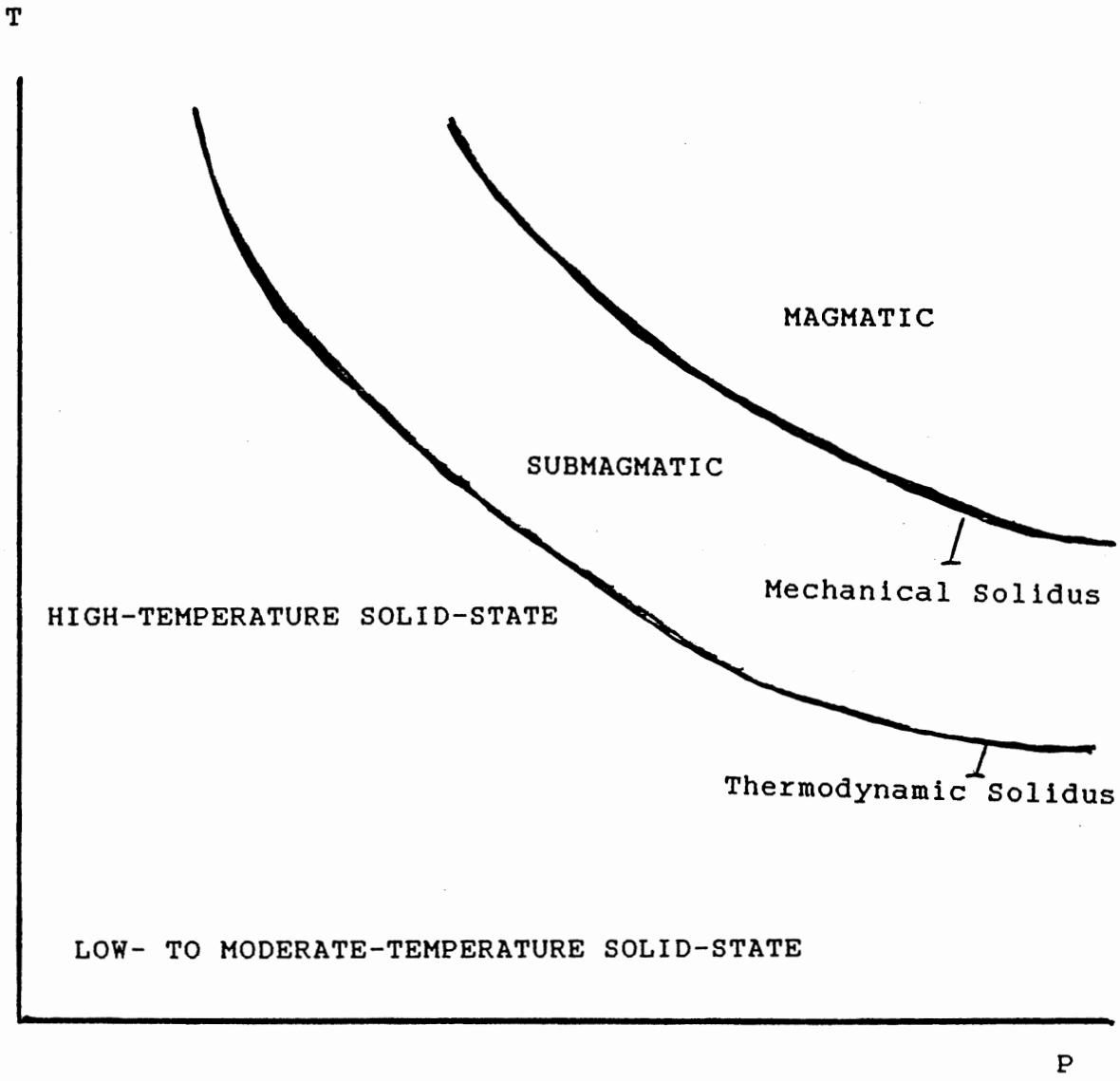

Figure 4.1 The general pressure-temperature conditions of foliation-producing processes.

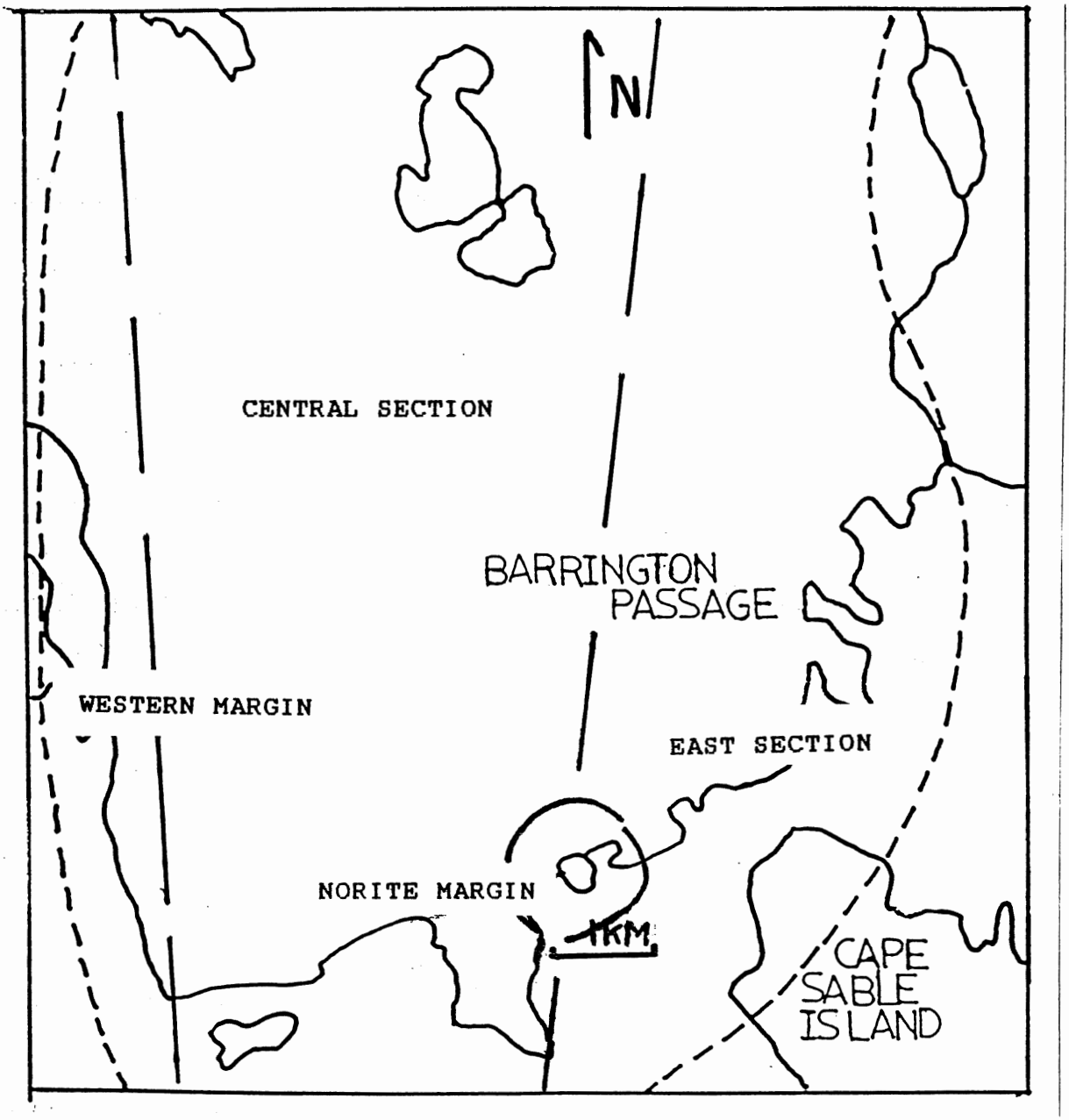

Figure 4.2 The distributions of the BPP sections for analysis of foliation criteria.

Table 4.1

Physical State	Melt > 25%	Melt < 25%	Melt=0	
Temperature Conditions	Magmatic Flow	Submagmatic Flow	High-Temperature Solid State Deformation	Low- to Medium-Temperature Solid State Deformation
Field Relations	foliations ‖ to contact [F]/ foliations more intense at contact [F]/ foliations bend around enclaves [F]/ igneous schlieren layering [F]/ convection lobes outlined [F]	compositional and structural zoning concentric in pluton [B]/ elongate pluton shape [ST]	cleavage triple-points at ends of pluton [ST]/ granitoid foliation continuous with wall rock foliation [ST]/ solid-state deformation in outer margins only [B]/ heterogeneous deformation (mylonite + ductile shear) [ST]	foliation by lenticular layering [T]/ foliation passes through enclaves [T]/ heterogeneous deformation (mylonite + ductile shear) [ST]
Contact Relations	foliations ‖ to contact [F+ST+B]	foliations ‖ to contact but not always ‖ to regional trend [B+F+ST]/ strong, elongate minerals rotated in wall rocks	wall rock foliation ‖ to contact [B]/ foliation ‖ to structural trend of region [ST]	granitoid foliation continuous with wall rock foliation [T]
Enclaves	preferred orientation [F]/ undeformed unless by flow shear [F]/ form screens near contact [F]	deformed, slightly less than host [B+ST]	deformed same as host [ST]/ deformed in solid-state at margins of granitoid only [B]	deformed same as host [T]
Pegmatites	--	deformed, folded towards margin [B]/ undulose extinction of quartz [all]	deformed, folded with host [T]/ deformed, folded at margins only [B]	deformed, folded with host granitoid [T]/ possibly boudinaged within host [T]
Aplites	--	deformed, folded towards margin, undeformed towards centre [B]/ deformed throughout [ST]	deformed, folded with host [ST]/ deformed, folded at margins only [B]	deformed, folded with host granitoid [T]
Microstructural Features (General)	primary igneous minerals and xenocrysts	possible magmatic recrystallization [B+ST]	microstructural heterogeneous deformation [M-SS]/ high-T porphyroblast growth [M-SS]	possible low-medium T porphyroblast growth [T]
Plagioclase	preferred orientation [F]/ imbrication [F]/ euhedral/ internal zoning/ growth twinning	rotation with possible supersolidus recrystallization [B+ST]	plasticallt elongated [ST] or fractured and broken [B]/ recrystallized, loses primary internal zoning [M-SS]/ rotation crystallization (porhyroblastic) [M-SS]	fractured with quartz in fractures [T]/ boudinaged [T]/ deformation twinning [T]/ plastic crystal slip [T]/ plastic deformation-> deformed inclusions.
Quartz	anhedral/ unoriented [F]/ euhedral in undeformed pegmatites	undulose extinction [B+ST]	c-slip deformation [M-SS]/ polygonized [M-SS]/ forms aggregates [ST+B]	forms dissolution veins [T]/ forms elongate ribbons or aggregates [T]/ a-slip deformation [T]
Alkali Feldspar	euhedral/ preferred orientation [F]/ development of myrmekite overgrowth	rotation with possible supersolidus recrystallization [B+ST]/ deformed myrmekite overgrowths [B+ST]	removal of myrmekite overgrowths except in pressure shadows [M-SS]	orthoclase inversion to microcline [T]/ boudinaged [T]
Biotite	subhedral to euhedral/ preferred orientation [F]	supersolidus deformation and recrystallization [B+ST]	alteration to chlorite [M-SS]	new, recrystyallized biotite [T]/ solid-state deformation into aggregates [T]/ deformational kinking [T]/ alter to chlorite

Letters in squared brackets refer to the process responsible for the feature. They represent:
T = Feature produced by tectonic/solid-state processes
ST = Feature produced by syntectonic emplacement processes
B = Feature produced by ballooning pluton processes
M-SS = Feature reflects transition from magmatic to solid-state processes. This includes ballooning and syntectonic processes.
F = Feature produced by magmatic flow processes

Table 4.1 A summary of the criteria of the foliation-producing processes.

foliations according to the four fields outlined. Some conditions may produce foliations during a transition from one process to another. The criteria outlined in Table 4.1 are generally those of Paterson et al.(1988), with some others included.

4.2.1 Methods of Pluton Emplacement

There are three methods of emplacing plutons, including emplacement by flow (convective diapiric rise), ballooning or inflation of a magma chamber, or syntectonic intrusion (exploitation of structural features or weak zones in the country rocks undergoing regional deformation). The latter two methods, ballooning and syntectonic intrusion, may produce foliations in granitoids under different conditions, because deformation may continue as the pluton cools, or two conditions (High-T Solid-State and Submagmatic) exist in the pluton at the same time.

Ballooning in plutons is a late-stage effect, occurring either by unroofing and inflation of the pluton or by successive injections of magma. Ballooning effects span conditions from magmatic at the centre, through submagmatic, to high-temperature solid-state deformation at the margins. As the magma chamber expands, the crystallized outer margins deform at near-solidus conditions while the central parts flow magmatically. Submagmatic conditions apply for the pluton itself, while high-temperature solid-state conditions apply to the outer margins and contact rocks.

Syntectonic emplacement involves the intrusion of granitoids during deformation. Intrusions exploit weaknesses in the host

rock, such as faults or shear zones, or structural features such as fold anticlines. Syntectonic emplacement implies that deformation continues as the pluton intrudes, as well as after it has cooled below the solidus. Criteria denoting syntectonic deformation reflect a transition of flow from magmatic to solid-state. Identification of subsolidus deformation requires care, because deformation must occur as the pluton cools, and is not the result of later overprinted deformation.

Both ballooning and syntectonic criteria are intermediate between the magmatic and tectonic end-members. The processes involving the individual criteria are defined in Table 4.1.

4.3.1 Characteristics of Magmatic Flow Foliations

Foliations produced by magmatic processes are the result of flow within the pluton involving the segregation of crystals by flow processes and "deformation by displacement of melt" (Paterson et al. 1988). Criteria for identifying magmatic foliations appear in Table 4.1. Magmatic foliations include the following:

1) Primary minerals have a preferred orientation. Elongated igneous minerals such as hornblende, feldspar, and biotite align parallel to the foliation. There must be enough melt to allow the crystals to align themselves without impediment from others.

2) Anhedral and unaligned quartz surrounds primary minerals. Undeformed quartz does not have a strong preferred orientation.

3) Imbrication of tabular minerals as a result of flow. Imbrication is a characteristic of flow, with crystals rotating

in a liquid. Tabular crystals in a flow imbricate themselves to minimize the resistance to the flow (Den Tex 1969). Imbrication must be distinguished from 'S-C' foliations produced in the solid-state, since both have similar appearances in granitic rocks.

4) Elongate enclaves orient parallel to the foliation. The enclaves may be either microgranitoids or country rock xenoliths. Elongation of enclaves is the result of shear produced by the flow of the surrounding magma, but also occurs as a result of solid-state deformation. Therefore the enclaves should show no signs of recrystallization or plastic deformation.

5) Foliations bend and bifurcate around enclaves and smaller microgranitoid enclaves also bend around large metasedimentary xenoliths.

6) Schlieren layering results from flow sorting and must be of igneous origin, with evidence indicating solid-state deformation absent. Solid-state deformation can include intense shearing of mafic dykes or recrystallized minerals composing the schlieren. Schlieren layering can also be the result of the automorphism and synneusis grouping of plagioclase, producing a swelling of the feldspar layer and compression of the biotite layer (Marre 1986).

7) Magmatic foliations are parallel to the pluton walls, as a result of cooler magma circulating back down into the magma chamber. Magmatic foliations may also outline separate convection lobes.

8) Foliation intensity increases toward the pluton margin.

Flattening of enclaves by flow shear and increased statistical alignment of primary minerals characterize this criterion.

9) The principal minerals must be primary and igneous. Features of primary igneous minerals include: euhedral crystal form, concentric zoning of plagioclase.

4.3.2 Characteristics of Submagmatic Flow Foliations

Criteria representative of this condition may result from either syntectonic or ballooning emplacement methods. A summary of these criteria appears in Table 4.1 and are as follows:

1) Ballooning emplacement of the pluton produces compositional zoning parallel to the contact. This results from the inward crystallization of the granitoid from the margins.

2) Like in magmatic flow-emplaced plutons, foliations are parallel to the contact.

3) Syntectonic intrusion produces an elongate pluton shape parallel to the structural orientation of the country rock.

4) Forces imposed on contact rocks by ballooning plutons or tectonic stresses on the pluton will result in rotation of wall rock foliations parallel to the contact.

5) Enclaves are solid bodies within crystal mush. The difference in material strength between the enclave and crystal mush accounts for the difference in deformation effects reflected in both.

6) Pegmatites and aplites intruded during ballooning of the pluton will undergo folding and deformation at the crystallized outer margins only.

7) Pegmatites and aplites intruding a crystal mush during tectonic deformation deform under the same circumstances as the host rock.

8) Submagmatic flow in a pluton only deforms quartz to the extent producing undulose extinction, because quartz is one of the last minerals to crystallize from a melt (Bowen 1928), and commonly occupies the interstitial spaces in the last stages of a cooling pluton.

9) Deformation resulting from both ballooning and syntectonic conditions induces rotation of strong minerals in both the pluton margin and contact margin.

10) Any recrystallization of minerals occurs under conditions above the thermodynamic solidus.

4.3.3 Characteristics of High-Temperature Solid-State Foliations

Both ballooning and syntectonic processes produce foliations under this condition. Criteria selected for this condition reflect deformation of the granitoid as it cools below the solidus, not deformation occurring during younger heating episodes. Criteria outlining high-teperature solid-state deformation are as follows:

1) Syntectonic stress applied under high temperature conditions will result in the formation of cleavage triple points at the ends of the pluton.

2) Stresses on syntectonic plutons produce an overprinted foliation parallel to the regional foliation trend.

3) If the margin of a ballooning pluton is completely solid then

deformation under this condition is expected.

4) Deformation is heterogeneous and results in the formation of ductile shear or mylonite zones bordering undeformed areas.

5) The wall rock foliation is parallel to the contact. This rotation occurring as a result of tectonic stress of the country rocks against the solid pluton, or ballooning pluton stress on the country rocks. In either case the high temperature makes the wall rocks relatively more ductile.

6) Pegmatite and aplite dykes intruded during regional deformation deform under the same conditions as the host pluton and have the same deformation characteristics.

7) Under ballooning conditions, pegmatite and aplite dykes deform at the solid outer margins only. The dykes originate at the core or molten parts of the magma chamber and cut the solid outer margins. Folding of a dyke in the outer margins of the pluton combined with no deformation of the same dyke at the centre is a characteristic of ballooning pluton deformation.

8) There are visible signs of heterogeneous deformation at the microstructural scale, with microscopic shear zones observed as planes of intensely recrystallized minerals such as biotite and quartz between more competent minerals like feldspars.

9) Synkinematic porphyroblasts grow in the contact rocks.

10) Plagioclase appears either plastically deformed as a result of high-temperature deformation or as fractured and rounded crystals, indicating brittle deformation under lower temperatures.

11) Plagioclase loses its primary concentric zoning during deformation. Plagioclase may also grow from rotation crystallization under high-temperature conditions, exhibiting the appropriate textures.

12) Quartz undergoes c-slip (molecular-scale crystal slip along the 'c' crystallographic axis) deformation, producing polygonized grains with subgrain textures.

4.3.4 Characteristics of Low- to Moderate-Temperature Solid-State (Tectonic) Foliations

Tectonically produced foliations involve many characteristics produced as a result of regional metamorphism or local deformation by shear zones. The deformation is plastic or brittle in nature and occurs in the solid state at low to moderate temperatures after pluton emplacement and cooling. The macro- and microstructural characteristics of foliations produced in low- to medium-temperature solid-state are as follows:

1) Minerals show evidence of plastic deformation including undulatory extinction of quartz and micas and kinks in feldspars and micas. This plastic deformation usually results in a reduction of grain size or the creation of aggregates and may also include development of metamorphic minerals. The new minerals are porphyroblasts, and they grow because conditions are favorable, and possibly the primary minerals are unstable and breaking down.

2) Formation of quartz "ribbons", or grain size reduction by α-

slip in crystals resulting in elongated aggregates.

3) Competent minerals such as feldspars or hornblende will undergo boudinage.

4) The inversion of orthoclase to microcline in the solid-state. Note that inversion of orthoclase to microcline also occurs under magmatic conditions at temperatures above the K-feldspar solidus. Therefore K-feldspar inversion must occur under solid-state conditions.

5) Foliations pass through enclaves because both enclaves and the host granitoid are solid. Ductility, and hence different states or very different rheologies are unlikely under the lower temperature conditions. Refraction of the foliation through the enclaves is possible if the enclave and surrounding granitoid have very different compositions.

6) Aplite dykes will deform and fold in the solid state as a result of plastic deformation. Determination must be made that the dyke folded in the solid-state and was not the result of folding during submagmatic flow.

7) Heterogeneous strain in the solid state results in the formation of mylonite shear zones or "microshear" zones at grain size scale.

8) Solid state (gneissic) foliations form lenticular bodies of recrystallized minerals. The foliation has an anastomosing and discontinuous nature. Fracturing of feldspars occurs at greenschist metamorphic facies and is a characteristic of solid-state deformation.

9) Two foliations (S-C foliations) form in response to dynamic deformation. S-C foliations meet at an angle of less than 35° and this angle decreases with increasing strain.

10) Some crystal solution occurs during the formation of solid-state foliations. Quartz and sulphide minerals will most easily go into solution, with these minerals being removed and reformed in planes parallel to the strain. Recrystallized quartz in pressure solution veins is coarser grained than igneous quartz and does not polygonize to the extent of primary quartz among the granitoids undergoing the same conditions (Burg and Ponce de Leon 1985).

11) Solid-state foliations match the regional foliation trend of the country rocks with little refraction of the foliations at the contact. Overprinting of previous magmatic foliations is possible, with both magmatic and tectonic foliations present. The tectonic foliation matches the regional trend, although the magmatic foliation may not.

12) Tectonic foliations are heterogeneous, because tectonic stresses exploit areas of weakness in the rock. This heterogeneity produces areas of intense deformation (mylonite zones) between less deformed areas.

13) Minerals producing the foliation should be recrystallized and neocrystallized minerals.

4.4 BPP Observations Related to Foliation Criteria

Each condition, and its application to the BPP follows in this section. Ballooning and syntectonic intrusion

characteristics replace the submagmatic and high-temperature solid-state conditions. Discussion of each of the emplacement modes relates to these conditions.

4.4.1 Magmatic foliations in the BPP

A summary of the data analysed appears in Table 4.2. Most of the criteria previously stated are visible to various degrees within the BPP with some criteria present throughout the pluton while others are present only at some locations.

Most foliation measurements of the BPP show that foliations are parallel to the contacts (Fig. 2.2) and mineral alignment is strongest in foliations closest to the contacts.

Foliation intensity increases towards the margins, as a rule, although foliation intensity can vary on an outcrop scale.

Deformation and strain on enclaves is difficult to determine, because the original shape is not known. Signs of deformation of enclaves within a flowage environment may include shortening of the enclave, shearing forces within a flow, or warping of metasedimentary xenoliths. Shortened enclaves (Fig. 2.9) and tailed enclaves (Fig. 2.8) occur in the BPP. The metasedimentary xenolith (Fig. 2.10) has a distinct bend that may be the result of ductile deformation within a flow, or possibly it is the original and undeformed shape of the xenolith.

Foliations do deflect around the enclaves of the BPP (Fig. 2.7). The deflection of the foliation is slight. Small enclaves bend with the foliation around larger enclaves (Fig. 2.11), implying that the enclaves can deform ductilely within magmatic

FEATURES	Western Margin	Central	Norite Margin	Eastern Margin
Foliation Parallel to contact	yes	no	no	yes
Intensity Increases Near Margin	NA	yes	NA	yes
Variable Foliation Orientation	yes(SH) no(WH)	yes	no	yes
Layered Schlieren	no	yes	no	yes
Flow Deformed Enclaves	NA	some	NA	yes
Foliation Bends Around Enclaves	NA	yes	NA	yes
Preferred Orientation of Enclaves	NA	yes	NA	yes
Aplites Structurally Undeformed	NA	yes	NA	yes
Pegmatites Structurally Undeformed	yes	yes	yes	yes
Undeformed Euhedral IgneousCrystals	no	yes	no	yes
Preferred Orientation in General	yes	yes	yes	yes
Preferred Orientation, Plagioclase	yes	yes	yes	yes
Preferred Orientation, Biotite	yes	yes	yes	yes
Preferred Orientation, K-Feldspar	yes	yes	yes	yes
Preferred Orientation, Others	hbl-no	no	no	hbl-yes
Anhedral, Undeformed Quartz	no	no	no	some
Imbrication	no	some	no	some

Table 4.2 BPP results relative to magmatic foliation criteria.

flow.

Elongate enclaves orient parallel to the foliation in the BPP. The only metasedimentary xenolith observed orients parallel to the foliation at location S10 (Fig. 2.10). Dark enclaves, inferred to be microgranitoids, are common in the eastern part of the study area. Thin section observations of the enclaves show that they have undergone minimal solid-state deformation. Some enclaves have a preferred orientation of biotite, orienting at an angle to the host rock foliation, suggesting that this enclave foliation predated the host foliation.

Schlieren layering is a common feature throughout the pluton and distinct schlieren bands are visible at various locations (Fig. 4.3).

Both aplites and pegmatites show only some recrystallization of quartz. There is no folding or bending of pegmatites observed.

Preferred orientation of elongate igneous minerals is present throughout the BPP. This preferred orientatation, especially of biotite and plagioclase, defines the foliation in the BPP. The percentage of elongate minerals, such as plagioclase and biotite aligned parallel to the foliation varies with the location. Biotite is the most consistently oriented mineral. Plagioclase alignment parallel to the foliation may vary from strongly aligned (Fig. 3.9) to weakly aligned (Fig. 4.4) within the pluton. Plagioclase is a primary mineral, as indicated by its euhedral shape and concentric internal zoning (Fig. 3.1).

Recrystallized aggregates of quartz surround most aligned

Figure 4.3 Schlieren banding, such as that shown at location S18, is common throughout the eastern margin and central sections of the pluton

Figure 4.4 Weak preferred orientation of plagioclase results in a weak foliation, such as at location S4. The scale of the photo is 20 mm across.

grains and also align parallel to the foliation (Fig. 3.7). Marre (1986) described quartz that has formed aggregates parallel to the flow direction in the Querigut Pluton in France, resulting from liquid filling interstitial spaces. The quartz aggregates described by Marre have a much larger grain size (~1mm) than the quartz aggregates of the BPP (~0.1mm). Paterson et al. (1988) noted that quartz is relatively sensitive to stress and will easily undergo plastic deformation.

There is inferred imbrication of minerals among the BPP samples. Inferred imbrication at some locations accounts for a preferred orientation of elongate plagioclase ~25° from that of the biotite orientation and dominant foliation (Fig. 3.4). Observations by Den Tex (1969) on ultramafic rocks revealed that the imbricated position of tabular crystals in a flow is the most stable position. The longest crystallographic axis of tabular minerals, β, orients subparallel to the flow and the short axis, α, is sub perpendicular to the flow direction (Den Tex 1969). Petrographic analysis of the fast and slow directions of individual crystals will determine their respective axes.

Field and petrographic studies of the BPP satisfy most of the criteria for flow-induced foliations. The strongest evidence in support of flow foliations include: the oriented enclaves and the bending of the foliations around these enclaves, the preferred orientation of primary minerals, schlieren layering, xenolith screens, and inferred imbrication of feldspars. However, magmatic flow foliations do not explain the recrystallized quartz

or the dynamic deformation of samples from the western and norite margins of the BPP.

4.4.2 BPP Observations Related to Ballooning Pluton Criteria.

Ballooning pluton criteria encompass both submagmatic and high-temperature solid-state conditions (Tables 4.3 and 4.4). Submagmatic conditions occur in the crystallizing margins of the pluton while high-temperature solid-state deformation occurs mainly in contact rocks. In the case of the norite margin, the BPP forms the country rock, while the norite occurs as the intrusion. This assumption forms the basis for analysis of ballooning pluton criteria. Evaluation of criteria pertains to the BPP, and analysis of the norite is limited to petrographic analysis of thin sections.

There is no zoning observed in the norite body. The only deformation observed is that of polygonized quartz. Pegmatites within the norite, both noritic and granitic in composition, show no signs of folding or other deformation except for the ubiquitous polygonized quartz.

Fractured and rotated plagioclase is common throughout the norite margin samples (Fig. 4.5). Plagioclase phenocrysts rotated in a solid-state as rigid bodies in a ductile matrix. Plagioclase crystals fractured and rounded as a result of collisions with other crystals (Fig. 4.6). Offsetting of the original foliation occured during this rotation, with the aligned biotite and quartz aggregates cut off or realigned (Fig. 4.7).

Inclusions in plagioclase possess no signs of deformation

Feature	Western Margin	Central	Norite Margin	Eastern Margin
Elongate Shape of Pluton (ST)	yes			
Compositional Zoning of Pluton (B)	no	no	no	no
Concentric Zoning of foliations (B)	no	no	yes	yes
Wall Rock Foliations Parallel Pluton Foliations (B+ST)	yes	NA	yes	yes
Deformed Enclaves,but Less Than Host (B+ST)	NA	yes	NA	yes
Pegmatites Folded Towards Margins (B)	NA	NA	NA	NA
Aplites Folded Towards Margins (B)	NA	NA	NA	no
Aplites/Pegmatites Deformed Throughout (ST)	NA	NA	NA	yes-qtz
Undulose Quartz in Pegmatites	no	no	no	no
Magmatic Recrystallization	no	no	no	no
Rotation of Feldspar in Pluton Margin (B+ST)	no	no	no	no
Rotation of Feldspar in Contact Margin (B+ST)	NA	NA	yes	NA
Undulose Quartz in Pluton Matrix (B+ST)	no	no	no	no
Myrmekite Deformation (B+ST)	NA	NA	NA	NA
Magmatic Recrystallization of Biotite (B+ST)	no	no	no	no

Table 4.3 BPP results according to submagmatic flow criteria

Features	Western Margin	Central	Norite Margin	Eastern Margin
Cleavage Triple Points at Pluton Ends (ST)	no	no	no	no
Pluton Foliation Continuous w/ Wall Rock (ST)	NA	NA	no	NA
Solid-State Deformation at Margins Only (B)	no	NA	yes	no
Heterogeneous Deformation (ST)	yes	no	yes	no
Wall Rock Foliation Rotated Parallel to Contact (B)	NA	NA	yes	NA
Enclaves Deformed Like Host Granitoid (ST)	NA	yes	NA	yes
Enclaves Deformed at Pluton Margins Only (B)	NA	NA	NA	no
Pegmatites/Aplites Deformed Like Host (ST)	no	yes	no	yes
Pegmatites/Aplites Deformed at Margins Only (B)	no	no	no	no
Microstructural Heterogeneous Deformation (B+ST)	yes	no	yes	no
High-Temperature/Synkinematic Porphyroblasts (ST)	no	no	no	no
Plastic Deformation of Plagioclase (ST)	some	no	no	no
Recrystallized/Rezoned Plagioclase (B+ST)	some	no	yes	no
Fractured Plagioclase (B)	yes	no	yes	no
Deformation of Quartz by c-slip (B+ST)	some	no	many	no
Polygonized Quartz	few	yes	few	yes
Pressure Shadows Around Strong Minerals (B+ST)	yes	no	yes	no

Table 4.4 BPP observations according to high-temperature solid-state criteria

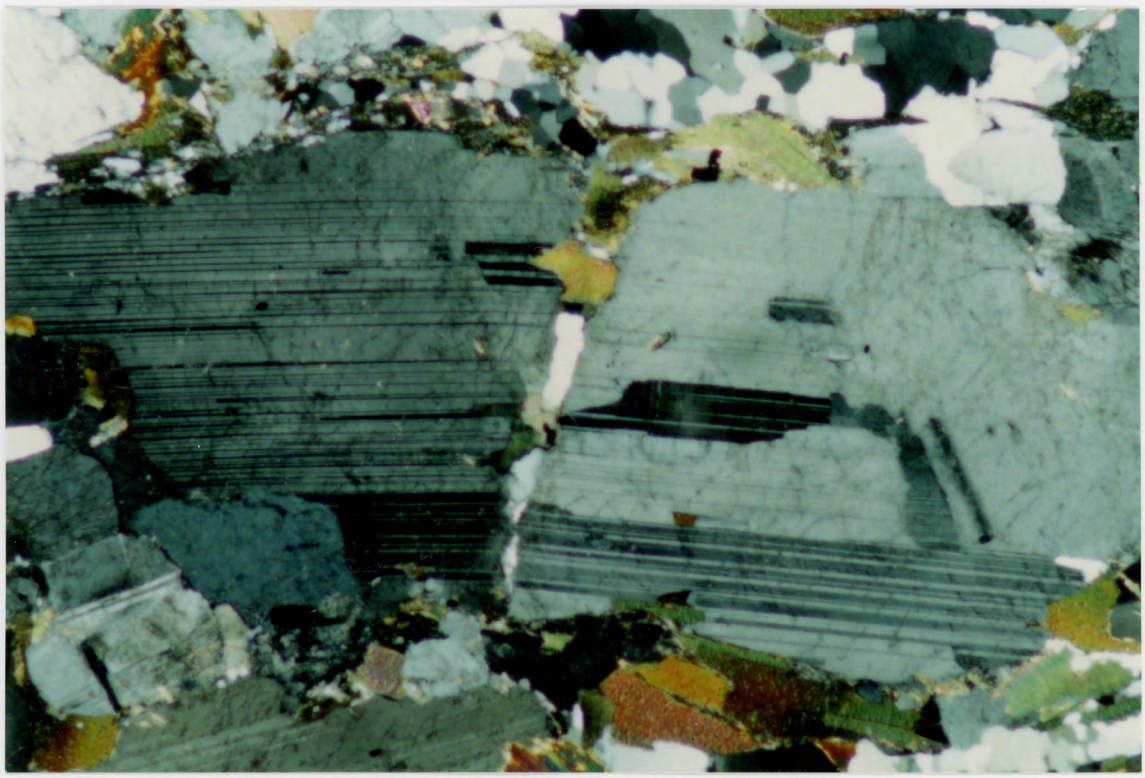

Figure 4.5 Fractured crystals commonly have more ductile minerals filling the fracture space. Quartz and biotite fill the fracture in this plagioclase crystal at location S15. The scale of the photo is 3 mm across.

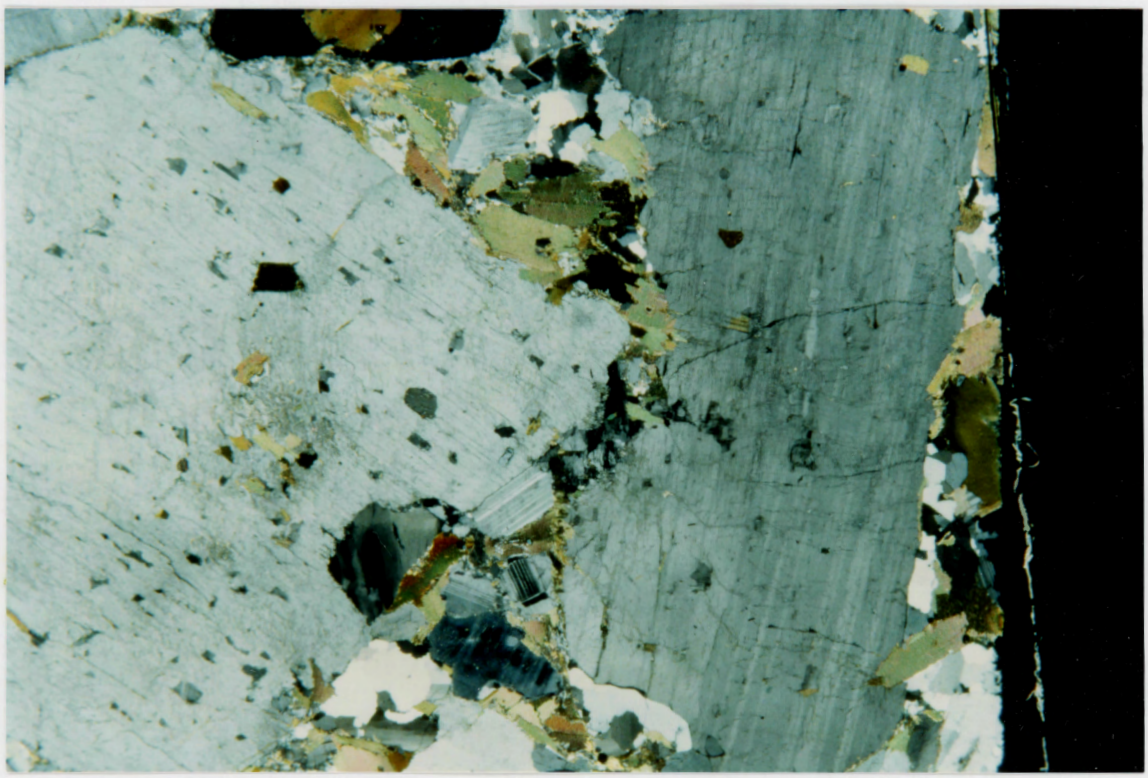

Figure 4.6 Plagioclase is a rigid mineral that will "float" among more ductile minerals during deformation. This sample, from location S15, shows the crystal interference that occurs during deformation, with an indication about the way feldspars are fractured in the solid-state. The scale of the photo is 10 mm across.

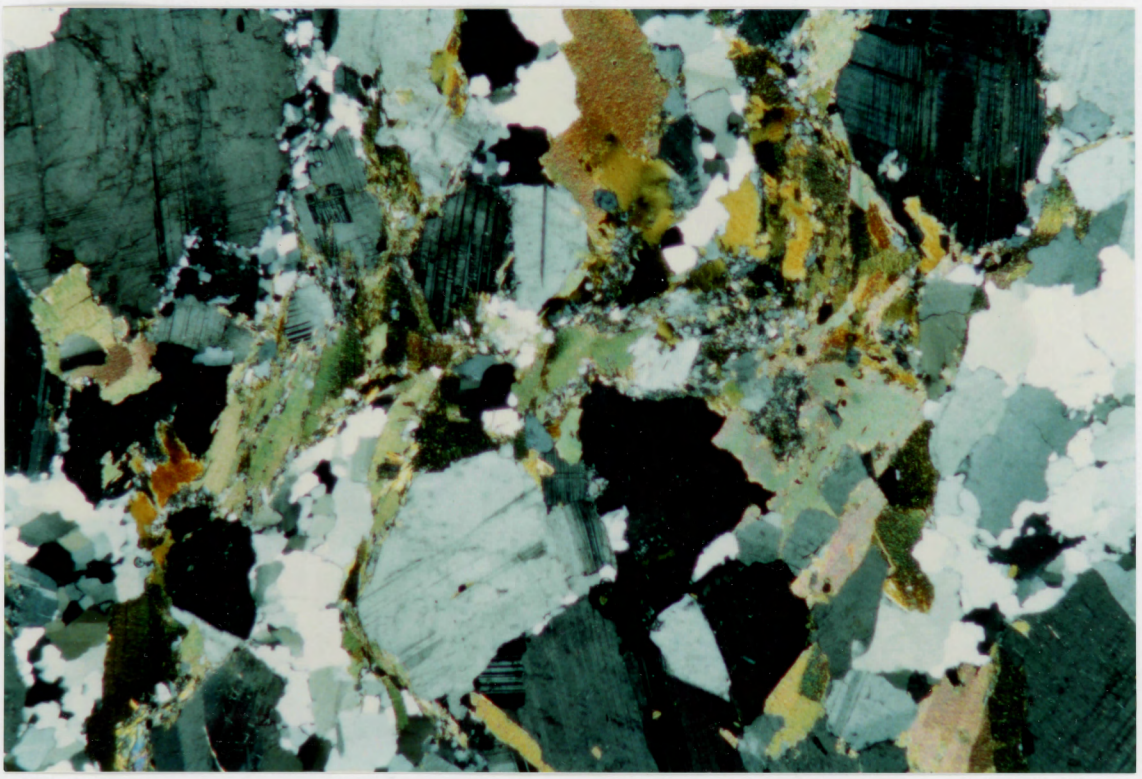

Figure 4.7 Deformation of the wall rocks includes a rotation of the foliation. Around the norite body, the foliation is offset and rotated, as shown in this sample from location S15. The original foliation has been rotated parallel to the norite-BPP contact. The scale of the photo is 5 mm across.

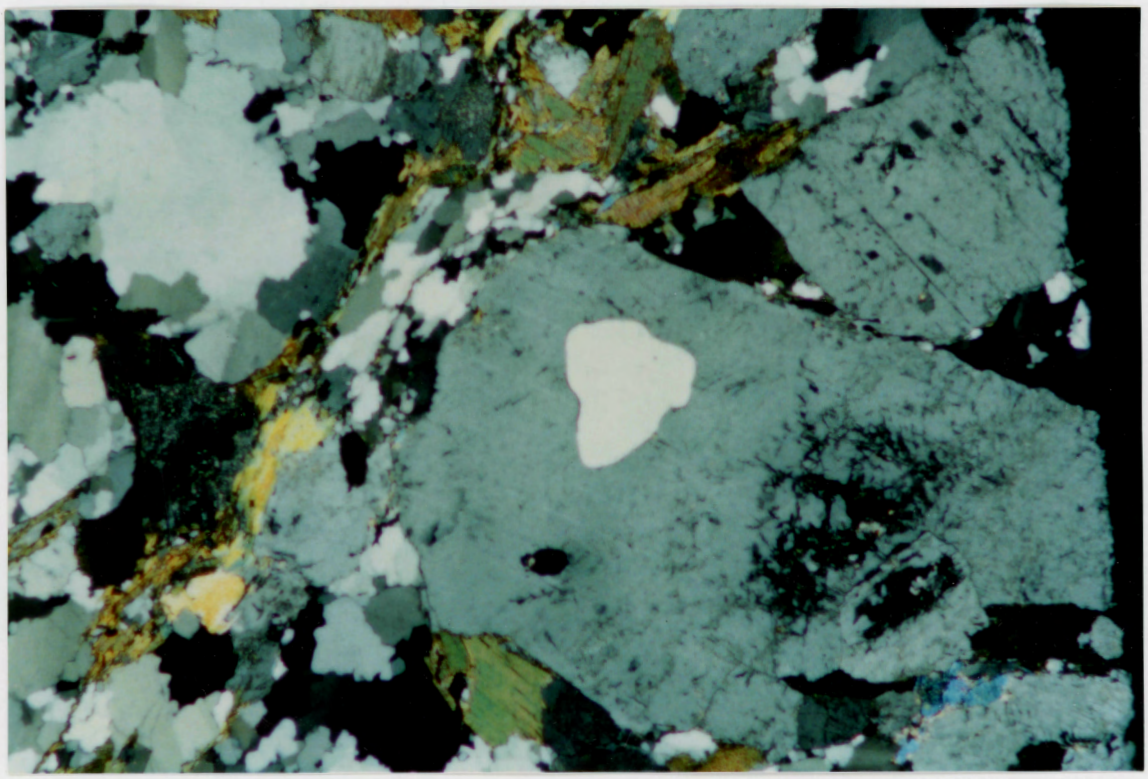

Figure 4.8 Inclusions in plagioclase will not deform if the plagioclase crystal is not ductilely deformed. The lack of deformation in this quartz inclusion indicates that the plagioclase host has not been deformed under ductile conditions. The scale of the photo is 6 mm across.

(Fig.4.8), indicating that only brittle deformation affected plagioclase instead of ductile deformation. Ductile deformation of plagioclase would affect the inclusions, creating polygonized or undulose extinction features in the quartz inclusions.

Microscopic shear zones between plagioclase crystals characterize the heterogeneous deformation. Fine-grained recrystallized biotite and quartz characterise these shear zones, with relatively undeformed tonalite on either side. These microstructural slip zones offset the primary foliation.

C-slip deformation is the dominant method influencing subgrain development in quartz. C-slip occurs at high temperatures, such as those occurring at the norite margin. Petrographic analysis of the fast and slow directions in quartz allows identification of the 'c' and 'a' crystallographic axes.

The intense alteration of the tonalite in the area surrounding the norite is the result of hydrothermal processes accompanying the intrusion of the norite. Hydrothermal alteration of the BPP accompanying the intrusion of the norite is a probable explanation for this alteration.

Development of the N-S foliations around the norite body may be the result of ballooning by the norite, or simply forceful intrusion of the norite into the BPP while it was still in a submagmatic condition. Possible rotation of the original magmatic foliation occurred during the norite emplacement. The foliations of the area are parallel to the inferred norite margin (Fig. 2.2).

Frost and Mahood (1987) discussed the influence of synplutonic mafic intrusions on a host granodiorite. Foliations in the granodiorite deflect around these mafic intrusions, and the mafic intrusions possess internal foliations. Age dating of the norite body produced an Rb/Sr date of 362 ± 18 my (de Albuquerque 1979), close to the BPP Ar/Ar age of 385 my (Reynolds et al. 1987) . This age indicates that the norite intruded soon after the emplacement of the BPP, or possibly as it cooled.

In summary, BPP emplacement probably was not by ballooning, but this process may explain the foliation orientation around the norite body. Solid state deformation of the margins and concentric zoning of the pluton is lacking, but there is sufficient evidence in favor of ballooning conditions affecting the BPP surrounding the norite body. Characteristics of the BPP surrounding the norite include realignment of foliations parallel to the norite contact, deformation of plagioclase in the BPP, heterogeneous deformation, and c-slip deformation of quartz. Ballooning does not explain why the norite does not have internal foliations or concentric zoning.

4.4.3 BPP Observations Relating to Syntectonic Emplacement Criteria

The long axis of the BPP is parallel to the structural trend of the country rocks. Most of the BPP foliations are parallel to the contact of the BPP and the Meguma Group rocks. Therefore, most foliations are parallel to the regional structural trend of the country rock but it is not known whether

structural trend of the country rock but it is not known whether the foliations of the BPP are continuous with the foliations in the country rocks. The contact orientation appears to control foliation orientation more than younger superimposed external forces.

The BPP has no internal cleavage, therefore cleavage triple points are not present.

Metamorphic isograds do grade away from the pluton to match the regional metamorphic trend (Fig. 1.2). The Meguma has undergone regional deformation to greenschist metamorphic facies, and contact metamorphism resulting from the intrusion of the BPP has raised the isograds up to sillimanite and migmatite grades near the contact. The isograds are concentric around the BPP.

The BPP is elongate in shape and orients parallel to one limb of a bend in the regional trend of the country rocks.

Paterson et al. (1988) note that syntectonic emplacement criteria should be used collectively rather than individually, because each feature can form as a result of other processes. Observations of the BPP indicate that tectonic forces probably did not influence the overall foliation produced in the BPP. Elongate shape of the BPP may indicate that it exploited a weak zone or regional anticline in the Meguma rocks. Regional tectonic deformation did not affect the pluton significantly during its intrusion although the deformation may be responsible for the recrystallizing of quartz throughout the BPP.

4.4.4 BPP Observations Relating to Tectonic (Low- to Moderate-Temperature Solid-state) Foliation Criteria

Table 4.5 summarizes the BPP observations according to tectonic foliation criteria. Some features of the BPP match the tectonic foliation criteria. Low- to moderate- temperature solid-state deformation conditions produced the gneissic foliations along the western margin.

There are no mylonite zones observed in the BPP but there is evidence of a shear zone along the western margin of the pluton. Samples taken from locations SH and WH have a gneissic texture defined by S-C foliations. S-C foliations have an anastomosing appearance defined by biotite alignment at an angle to the preferred plagioclase alignment (Fig. 2.6). There are biotite lineations within the foliation plane and the lineations are subhorizontal, indicating a relative dextral motion for this shear zone.

The foliation intensity in the BPP is heterogeneous and is attributable to magmatic flow. The gneissic foliation at location WH and SH is probably the result of a local shear zone. The gneissic foliations at WH and SH 1-3 are the only foliations attributable to plastic deformation in the solid-state.

S-C foliations are present only in the gneissic foliation at location WH and no S-C foliations appear in the SH samples because the sample area may be farther from the most deformed part of the shear zone. There is no development of S-C planes elsewhere in the BPP.

Feature	Western Margin	Central	Norite Margin	Eastern Margin
Lenticular Layering	yes	no	some	no
Foliation Passes Thru Enclaves	NA	no	NA	no
Heterogeneous Deformation	yes	no	yes	no
S-C Foliations	yes	no	no	no
Mutual Deformation of Granitoids and Regional Structures	yes	NA	NA	NA
Foliation Continuous w/ Wall Rocks	NA	NA	no	NA
Enclaves Deformed Like Host	NA	no	no	No
Pegmatites Deformed Like Host	no	some-qtz	no	some-qtz
Aplites Deformed Like Host	NA	no	no	no
Low Temperature Porphyroblasts	no	no	no	no
Quartz Filling in Plagioclase Fractures	yes	no	yes	no
Plastic Deformation of Plagioclase	yes	no	no	no
Solid-State Rotation of Plagioclase	yes	no	yes	no
Dissolution of Primary Minerals	yes	no	no	no
Quartz Forms Aggregates or Ribbons	yes	yes	yes	yes
Quartz Undergoing α-slip	some	no	yes	no
Orthoclase = > Microcline	yes	yes	yes	yes
Boudinage of Strong Minerals	no	no	no	no
Recrystallized Biotite	yes	no	yes	no
Deformation of Biotite to Aggregates	yes	no	yes	no
Deformation Kinks in Biotite	some	no	few	no
Deformation of Inclusions	some	no	no	no

Table 4.5 BPP observations according to low- to moderate-temperature deformation criteria

Foliations bend around enclaves with no sign of the foliation passing through enclaves anywhere in the BPP. There are no enclaves observed in the deformed areas. Deformed microgranitoid enclaves do not make good indicators of solid-state deformation because they also deform under flow conditions (Vernon et al. 1988).

There were no aplite dykes observed in the western margin section during field studies and deformation of other secondary intrusions such as pegmatites is minimal.

Samples from the BPP possess polygonized and recrystallized quartz throughout the pluton. Larger quartz grains have internal polygonal subgrain boundaries but most quartz recrystallizes into aggregates of small, equant grains.

The western margin samples show signs of exsolution defined by the segregation of opaque minerals from biotite. Opaque minerals occur as inclusions in biotite at all other locations in the BPP, but at location WH and SH, opaque minerals occur only at the margins of biotite. Epidote, titanite, and rutile occur along the cleavage traces in the SH samples suggesting that exsolution of these minerals is not complete. The segregation of inclusions in biotite may be the result of dynamic deformation.

Quartz recrystallized into aggregates and "ribbons" are common throughout the BPP. Samples from both the margins and the centre of the pluton contain quartz ribbons. Quartz aggregates combine with biotite at location WH to impart a lenticular pattern of biotite and quartz surrounding large plagioclase

phenocrysts.

Plastic deformation of plagioclase and biotite occurs at locations from the western margin of the pluton. Fracturing of plagioclase and alteration of biotite to chlorite has occurred in this area. Recrystallized quartz and biotite fill in the fractures in plagioclase, in much the same way as the fractures in plagioclase from the norite margin are filled (Fig. 4.5). Plagioclase also exhibits evidence of plastic deformation defined by bent polysynthetic twins (Fig. 3.3) and deformed inclusions. Plastic deformation of plagioclase indicates a significant stress imposed on the rocks. Deformation of plagioclase to this extent occurs only in the western sample areas. Deformation of plagioclase by fracturing occurs at greenschist metamorphic grade conditions (moderate temperature) (Paterson et al. 1988)

K-feldspar comprises less than 5% of the BPP tonalite and occurs only in the form of microcline. Inversion of orthoclase to microcline can also occur under magmatic conditions, as the temperature drops closer to the K-feldspar solidus. The inversion of orthoclase to microcline is assumed to be complete in the BPP.

Boudinage of competent minerals is not present. Hornblende is not significantly plentiful for assessment of deformation.

The minerals producing the foliation in the BPP are primary magmatic and, other than quartz there is no evidence of widespread recrystallization in the study area. Except for quartz, there is no widespread plastic deformation of the primary igneous minerals. Recrystallized aggregates of quartz occur at

all locations. This recrystallization of quartz is possibly in response to a younger and weak deformation event, since this strain does not affect other primary minerals.

One late-stage brittle fault occurs in the BPP at location HW. This brittle faulting happened when the pluton was in solid-state and fault gouge characterizes brittle deformation. Forces responsible for this faulting do not influence the primary foliation.

Deformation along the western margin is the result of a shear zone. This shearing would have occurred as the pluton cooled to moderate temperatures. Deformation of the rock at WH would require moderate temperatures. Shearing is in response to relative strike-slip motion between the BPP and the country rock. Analysis of biotite lineations in sample WH, provided the directional component for the shear.

Tectonic solid-state processes are responsible for producing a foliation in only one area. The gneissic foliation at locations WH and SH 1-3 is the result of a shear zone near or at the contact between the BPP and the country rock.

The only similarity between the foliations of the BPP and the regional trend is the common orientation. Not all the foliations of the pluton match the regional trend. The plutonic foliations are parallel to the contacts. The BPP foliations are magmatic in origin, and any similarity with the surrounding tectonically-derived structural trend is coincidental.

The only features attributable to low to moderate

quartz and the shear zone along the western margin. Foliations at all other locations are the result of magmatic flow. Deformation of the central and eastern margin sections of the pluton was not strong enough to overprint the magmatic foliation or develop a solid-state foliation.

4.5 Synthesis and Conclusions

The foliations in the undeformed central and eastern margin sections of the pluton are magmatic in origin. Genesis of this foliation during the magmatic phase and the result of flow within the pluton. Schlieren layering, preferred orientation of primary minerals, and foliations deflecting around enclaves strongly support a magmatic flow origin for the foliation.

Ballooning processes deformed the tonalite around the norite body. Realignment of the foliation parallel to the norite contact, heterogeneous deformation of the tonalite, and recrystallized plagioclase all support this process. Emplacement of the norite occurred soon after the the emplacement of the BPP. The forces required to deform the BPP to this extent would not be as great if the pluton was still at a high temperature because deformation occurs more easily at high temperatures than lower temperatures. The shear strength of a rock decreases with temperature increase, and likewise, the shear strength decreases with the increasing melt content of a rock (Arzi 1978).

The shear zone along the western margin possesses the characteristics of moderate-temperature solid-state deformation. Criteria such as S-C foliations, heterogeneous deformation,

Criteria such as S-C foliations, heterogeneous deformation, recrystallized primary minerals, plastic deformation of plagioclase, and segregation of opaque minerals from biotite characterize solid-state deformation in a shear zone. This shear zone is the result of movement between the BPP and country rocks or a regional shear cutting both the country rock and the pluton.

The BPP most likely exploited and intruded a fault system or structural feature resulting from the Acadian Orogeny. Intrusion of granitoids into active shear zones is well documented. Rotation of plutons occurs within large tectonic shear zones, with subsequent shortening of plutons and associated deformational features (Castro 1986). Extensional shear zones and wrench faults provide a weak point in the crust for magma intrusions, with the plutons commonly oriented perpendicular to the extension direction (Hutton et al. 1990). This theory does not apply to the BPP because the pluton intruded in the late stages of a compressional orogeny. Intrusion of the BPP was late in the Acadian Orogeny or after the main phase of deformation.

The BPP dates at 385 Ma (Ar/Ar) (Reynolds et al. 1985). It should be noted that U/Pb dates are more effective for emplacement ages, while Ar/Ar dates are best used to determine the metamorphic events (Paterson et al. 1989).

Shear zones occur throughout the area, and movement along these shear zones continued well after the Acadian Orogeny. Triassic dykes are offset in the region as a result of these shear zones, implying that shear zones have developed after the

emplacement of the BPP. The shear zone of the west margin of the BPP is likely to have started deforming the BPP after the pluton had cooled below the thermodynamic solidus. Dating of micas from two nearby shear zones indicate that movement postdated the BPP intrusion (~320 my and ~280 my Dallmeyer and Keppie 1986).

Recrystallization of quartz is an overprinting feature. This deformation postdates the emplacement of the BPP. In coarse grained rocks such as granites, recrystallized quartz aggregates align parallel to the foliation (Paterson et al. 1989). The quartz in pegmatites and enclaves underwent less deformation than that of the host tonalite. The pegmatites might have intruded after much of the deformation passed, or the pegmatites could relate to another later thermal event in the region, as suggested by Reynolds et al. (1987). Due to the fine-grained texture of the enclaves, deformation of quartz within them may not be to the same extent as that of the quartz in the host tonalite.

Chapter 5

Conclusions

- The original foliation in the BPP is of magmatic origin. Plagioclase and biotite alignment define the foliation. Schlieren layering, alignment of enclaves with the flow direction, bifurcation of the foliation around enclaves, preferred orientation of primary igneous minerals, imbrication of plagioclase, foliations parallel to the contact, and variable intensity and orientation characterizes a foliation of magmatic origin.

- A shear zone deforms the western margin of the BPP. S-C foliations, lenticular layering, heterogeneous deformation, fracturing and rotation of plagioclase, plastic deformation of plagioclase, recrystallization of quartz and biotite, and alignment of quartz aggregates within the foliation indicate deformation at moderate temperatures. The shear zone formed under moderate-temperature deformation conditions, as the pluton cooled.

- Deformation of the BPP around the norite body occurred under circumstances similar to those of deformation resulting from ballooning plutons. Rotation of the primary magmatic foliations parallel to the norite contact, rotation and deformation of plagioclase in the wall rock (BPP), hydrothermal alteration of the tonalite, microstructural heterogeneous deformation, and c-

slip in quartz suggest that the BPP deformed as a result of the norite intrusion. At high temperatures, granitoids undergo deformation more readily, therefore, ballooning of the norite body may not have had to occur. Forceful diapiric rise produces the same effects.

- Syntectonic effects on the BPP are minimal. Small residual stresses from the Acadian Orogeny recrystallized the quartz throughout the study area. The small amount of stress exerted on the BPP only caused deformation in quartz which aligned parallel to the foliation.

- Table 5.1 contains a summary of the events relative to the intrusion of the BPP.

Recommendations for Further Work

A more detailed study of the contact relations between the BPP and the Meguma Group would allow precise identification of the method of emplacement or tectonic deformation setting.

Analysis of the norite body and its contact with the BPP will produce conclusive results as to its origin and nature, along with the exact effect it had on the BPP.

Sampling along a north-south strike may document some chemical variation, because the surficial shape of the pluton suggests that the northern part of the pluton is not as deeply eroded as the southern part.

Investigation of anomalous lineaments observed on aeromagnetic vertical gradient maps of the area may yield new and important features.

Relative Time	Event
↑	Slight,residual deformation deforming quartz
|	Shearing along western margin
|	Norite intrusion and annealing of tonalite
|	End of moderate to light deformation
|	Formation of magmatic foliation
|	Intrusion and emplacement of BPP
|	Main phase of Acadian deformation

Table 5.1 Summary of Significant Events Related to the Production of Foliations in the BPP

Appendix A Sample Petrography

	Sample S1	Sample S2	Sample S2b
Sample Location	roadcut	roadcut, 500m south of location 1	roadcut
Sample Description	biotite tonalite	biotite tonalite	border around enclave
Modal % Plagioclase	50	55	45
Modal % Biotite	15	15	30
Modal % Quartz	32	25	20
Modal % K-Feldspar	<3	5	<5
Other Minerals	apatite, titanite, hornblende, epidote,	apatite, epidote	apatite, epidote
Foliation Strength	strong	moderate	weak
Deformation Characteristics	minor deformation of quartz	minor deformation of quartz	very minor deformation of quartz

Appendix A (continued)

	Sample S2c	Sample 3	Sample 4
Sample Location	roadcut	roadcut, 20m south of S2	new stone quarry
Sample Description	enclave	biotite tonalite	biotite tonalite
Modal % Plagioclase	10	50	50
Modal % Biotite	35	20	20
Modal % Quartz	20	20	25
Modal % K-Feldspar	0	<10	<5
Other Minerals	hornblende (35%), epidote	apatite, epidote	apatite
Foliation Strength	not foliated	moderate	moderate
Deformation Characteristics	very minor weathering	recrystallized quartz in aggregates	polygonized quartz

Appendix A (continued)

	Sample S5	Sample S6	Sample S7
Sample Location	new stone quarry	new stone quarry	new stone quarry
Sample Description	biotite tonalite	biotite tonalite	biotite tonalite
Modal % Plagioclase	50	50	50
Modal % Biotite	20	15	20
Modal % Quartz	25	35	25
Modal % K-Feldspar	<5	0	<5
Other Minerals	opaque minerals	epidote, apatite	epidote
Foliation Strength	moderate	weak-moderate	moderate
Deformation Characteristics	polygonized quartz	highly polygonized quartz	some weathering, polygonized quartz

Appendix A (continued)

	Sample S8	Sample S9	Sample S10
Sample Location	new stone quarry	new stone quarry	Shag Harbour
sample Description	biotite tonalite/ granitic dyke	biotite tonalite/ felsic injections	biotite tonalite
Modal % Plagioclase	50/10	50/60	50
Modal % Biotite	20/5	15/0	15
Modal % Quartz	25/30	30/30	30
Modal % K-Feldspar	<5/50	<5/10	5
Other Minerals	epidote/ muscovite (5%)	epidote	epidote, apatite, titanite
Foliation Strength	weak/not foliated	weak/not foliated	strong
Deformation Characteristics	polygonized quartz/ no deformation	polygonized quartz/ no deformation	recrystallized quartz in aggregates

Appendix A (continued)

	Sample S11	Sample S12	Sample S13
Sample Location	west of Doctors point	east of Doctors Point, Murray Cove	east of Doctors Point, Murray Cove
Sample Description	biotite tonalite	biotite tonalite	biotite tonalite
Modal % Plagioclase	45	55	50
Modal % Biotite	20	5	15
Modal % Quartz	30	30	30
Modal % K-Feldspar	5	10	<5
Other Minerals	muscovite, epidote, apatite	sericite, opaque minerals	sericite, opaque minerals
Foliation Strength	weak	moderate	moderate
Deformation Characteristics	polygonized quartz	extensive alteration of plagioclase, polygonized quartz	extensive alteration of plagioclase, polygonized quartz

Appendix A (continued)

	Sample S14	Sample S15	Sample S16
Sample Location	west of Barrington Passage, Murray Cove	50 m east of Sample S14	Murray Cove
Sample Description	biotite tonalite	biotite tonalite	biotite tonalite
Modal % Plagioclase	45	50	55
Modal % Biotite	20	15	10
Modal % Quartz	30	30	25
Modal % K-Feldspar	<5	<5	10
Other Minerals	muscovite, epidote	epidote	opaque minerals
Foliation Strength	moderate	moderate	moderate
Deformation Characteristics	recrystallized quartz in aggregates, fractured plagioclase	recrystallized quartz in aggregates, fractured plagioclase	extensive alteration of plagioclase, polygonized quartz

Appendix A (continued)

	Sample S17	Sample S18	Sample SH (1,2,3)
Sample Location	old stone quarry	Penney Estates, Cape Sable Island	north of Shag Harbour
Sample Description	biotite tonalite	biotite tonalite	biotite tonalite
Modal % Plagioclase	50	55	50
Modal % Biotite	15	15	20
Modal % Quartz	20	25	25
Modal % K-Feldspar	<10	<5	<5
Other Minerals	epidote	epidote	chlorite, opaque minerals
Foliation Strength	moderate	moderate	gneissic
Deformation Characteristics	polygonized quartz	polygonized quartz	recrystallized quartz in aggregates, gneissic foliation

Appendix A (continued)

	Sample WH	Sample HW	Sample O/C-9
Sample Location	north of Woods Harbour	northeast of Oak Park Lake	200 m east of Sample S12
Sample Description	biotite tonalite	biotite tonalite	granite pegmatite
Modal % Plagioclase	60	50	15
Modal % Biotite	15	15	<5
Modal % Quartz	20	30	20
Modal % K-Feldspar	5	<5	>60
Other Minerals	opaque minerals, chlorite	epidote	muscovite
Foliation Strength	gneissic	weak	not foliated
Deformation Characteristics	gneissic foliation, fractured and deformed plagioclase, quartz aggregates	polygonized quartz	not deformed

Appendix A (continued)

	Sample OQX (1,4)	Sample OQX (2,3)	Sample OQV (1,2)
Sample Location	old stone quarry	old stone quarry	old stone quarry
Sample Description	enclave	enclave	igneous vein
Modal % Plagioclase	40	40	50
Modal % Biotite	50	50	<5
Modal % Quartz	10	10	35
Modal % K-Feldspar	0	0	10
Other Minerals	epidote	epidote	epidote(~1%)
Foliation Strength	not foliated	moderate	not foliated
Deformation Characteristics	minor polygonized quartz	polygonized quartz	polygonized quartz

Appendix A (continued)

	Sample N1	Sample N2	Sample N3
Sample Location	norite outcrop, Murray Cove	norite outcrop, Murray Cove	norite outcrop, Murray Cove
Sample Description	gabbronorite	gabbronorite	gabbronorite
Modal % Plagioclase	45	40	30
Modal % Biotite	<5	0	5
Modal % Quartz	0	5	0
Modal % K-Feldspar	10	0	0
Other Minerals	clinopyroxene 25%, orthopyroxene 20%	clinopyroxene 30%, orthopyroxene 25%	clinopyroxene 35%, orthopyroxene 30%
Foliation Strength	not foliated	not foliated	not foliated
Deformation Characteristics	not deformed	not deformed	not deformed

Appendix A (continued)

	Sample N4	Sample N5	Sample N6
Sample Location	norite outcrop, Murray Cove	norite outcrop, Murray Cove	norite outcrop, Murray Cove
Sample Description	gabbronorite	gabbronorite	granitic pegmatite
Modal % Plagioclase	55	45	10
Modal % Biotite	5	0	5
Modal % Quartz	0	0	15
Modal % K-Feldspar	0	0	60
Other Minerals	clinopyroxene 25%, orthopyroxene 15%	clinopyroxene 30%, orthopyroxene 25 %	muscovite 5%, magnetite 5%
Foliation Strength	not foliated	not foliated	not foliated
Deformation Characteristics	not deformed	not deformed	undulose quartz

Appendix A (continued)

	Sample N7
Sample Location	norite outcrop, Murray Cove
Sample Description	noritic pegmatite
Modal % Plagioclase	50
Modal % Biotite	0
Modal % Quartz	5
Modal % K-Feldspar	0
Other Minerals	Clinopyroxene 35%, orthopyroxene 15%
Foliation Strength	not foliated
Deformation Characteristics	not deformed

Appendix B Chemical Data for Plagioclase

Sample	N1	N1	N1	S1
Analysis	0040	0041	0046	0001
Location	CORE	RIM	RIM	CORE
Mineral	PLA	PLA	PLA	PLA
SiO2	57.75	55.52	56.69	59.59
Al2O3	26.76	28.35	26.21	25.36
CaO	9.24	10.60	7.87	6.89
Na2O	6.35	5.69	7.45	8.13
K2O	0.08	0.00	0.12	0.05
Total	100.18	100.16	98.34	100.02
Si	10.328	9.978	-	10.634
Al	5.636	6.001	-	5.330
Ca	1.771	2.041	-	1.317
Na	2.202	1.983	-	2.813
K	0.018	0.000	-	0.011
SUM CATS	19.955	20.004	-	20.105
Z	15.96	15.98	-	15.96
X	3.99	4.02	-	4.14
Ab	55.17	49.27	-	67.92
An	44.37	50.73	-	31.81
Or	0.46	0.00	-	0.27

Sample	S1	S1	S1	S1
Analysis	0002	0005	0006	0037
Location	RIM	CORE	RIM	RIM
Mineral	PLA	PLA	PLA	PLA
SiO2	58.82	60.87	61.30	60.10
Al2O3	21.28	24.89	24.24	25.28
CaO	6.55	6.57	6.46	6.84
Na2O	8.50	8.39	8.20	7.82
K2O	0.00	0.00	0.02	0.00
Total	95.15	100.72	100.22	100.10
Si	-	10.766	10.877	10.695
Al	-	5.185	5.065	5.299
Ca	-	1.245	1.228	1.304
Na	-	2.877	2.821	2.698
K	-	0.000	0.005	0.000
SUM CATS	-	20.073	19.996	19.997
Z	-	15.95	15.94	15.99
X	-	4.12	4.05	4.00
Ab	-	69.80	69.59	67.41
An	-	30.20	30.30	32.59
Or	-	0.00	0.11	0.00

Sample	S1	S10	S10	S10
Analysis	0038	0008	0009	0010
Location	CORE	RIM	CORE	RIM
Mineral	PLA	PLA	PLA	PLA
SiO2	58.96	60.21	61.27	61.68
Al2O3	25.23	25.01	24.30	24.59
CaO	7.33	6.89	5.85	6.27
Na2O	7.81	8.29	8.78	7.88
K2O	0.00	0.06	0.04	0.15
Total	99.33	100.46	100.24	100.57
Si	10.602	10.698	10.873	10.887
Al	5.343	5.233	5.079	5.112
Ca	1.412	1.312	1.112	1.186
Na	2.723	2.856	3.021	2.697
K	0.000	0.014	0.009	0.034
SUM CATS	20.080	20.112	20.095	19.915
Z	15.94	15.93	15.95	16.00
X	4.14	4.18	4.14	3.92
Ab	65.85	68.30	72.93	68.86
An	34.15	31.37	26.85	30.28
Or	0.00	0.33	0.22	0.86

Sample	S10	S10	S11	S11
Analysis	0011	0012	0022	0023
Location	CORE	RIM	CORE	RIM
Mineral	PLA	PLA	PLA	PLA
SiO2	61.48	60.12	62.29	59.84
Al2O3	24.32	25.30	24.73	24.88
CaO	6.20	7.28	6.09	6.21
Na2O	8.23	7.85	8.52	8.47
K2O	0.03	0.01	0.00	0.00
Total	100.26	100.56	101.63	99.40
Si	10.893	10.664	-	10.725
Al	5.075	5.286	-	5.252
Ca	1.177	1.384	-	1.193
Na	2.827	2.700	-	2.943
K	0.007	0.002	-	0.000
SUM CATS	19.979	20.036	-	20.113
Z	15.97	15.95	-	15.98
X	4.01	4.09	-	4.14
Ab	70.49	66.08	-	71.17
An	29.34	33.87	-	28.83
Or	0.17	0.06	-	0.00

Sample	S11	S11	S11	S11
Analysis	0024	0025	0026	0027
Location	CORE	RIM	CORE	RIM
Mineral	PLA	PLA	PLA	PLA
SiO2	62.19	58.57	60.57	59.53
Al2O3	24.89	25.04	25.20	25.88
CaO	6.25	6.32	6.61	7.57
Na2O	8.10	8.49	8.10	7.76
K2O	0.00	0.00	0.00	0.00
Total	101.43	98.42	100.48	100.74
Si	10.878	-	10.730	10.556
Al	5.128	-	5.258	5.405
Ca	1.171	-	1.255	1.438
Na	2.747	-	2.782	2.668
K	0.000	-	0.000	0.000
SUM CATS	19.924	-	20.024	20.067
Z	16.01	-	15.99	15.96
X	3.92	-	4.04	4.11
Ab	70.11	-	68.92	64.97
An	29.89	-	31.08	35.03
Or	0.00	-	0.00	0.00

Sample	S15	S15	S15	S15
Analysis	0030	0031	0032	0033
Location	CORE	RIM	CORE	RIM
Mineral	PLA	PLA	PLA	PLA
SiO2	61.17	61.73	61.27	61.50
Al2O3	24.36	24.68	24.94	24.49
CaO	6.07	6.26	6.37	6.28
Na2O	8.20	8.33	8.42	8.09
K2O	0.00	0.00	0.06	0.03
Total	99.80	101.00	101.06	100.39
Si	10.882	10.860	10.792	10.879
Al	5.104	5.114	5.174	5.102
Ca	1.157	1.180	1.202	1.190
Na	2.829	2.842	2.876	2.775
K	0.000	0.000	0.013	0.007
SUM CATS	19.972	19.996	20.058	19.953
Z	15.99	15.97	15.97	15.98
X	3.99	4.02	4.09	3.97
Ab	70.97	70.66	70.29	69.86
An	29.03	29.34	29.38	29.97
Or	0.00	0.00	0.33	0.17

Sample	S15	S15	S17	S17
Analysis	0034	0035	0050	0051
Location	CORE	RIM	CORE	RIM
Mineral	PLA	PLA	PLA	PLA
SiO2	59.24	61.58	58.92	60.59
Al2O3	25.74	25.15	26.21	25.14
CaO	7.27	6.66	8.07	6.79
Na2O	7.97	8.22	7.56	8.14
K2O	0.00	0.00	0.00	0.00
Total	100.22	101.64	100.76	100.66
Si	10.560	-	10.465	10.724
Al	5.404	-	5.483	5.240
Ca	1.389	-	1.536	1.288
Na	2.755	-	2.604	2.793
K	0.000	-	0.000	0.000
SUM CATS	20.107	-	20.087	20.045
Z	15.96	-	15.95	15.96
X	4.14	-	4.14	4.08
Ab	66.49	-	62.90	68.45
An	33.51	-	37.10	31.55
Or	0.00	-	0.00	0.00

Sample	S17	S17	S17	S17
Analysis	0052	0053	0054	0055
Location	CORE	RIM	CORE	RIM
Mineral	PLA	PLA	PLA	PLA
SiO2	59.64	58.32	58.94	57.99
Al2O3	25.84	25.47	26.30	26.24
CaO	7.73	6.76	8.41	8.00
Na2O	7.50	7.95	7.06	7.37
K2O	0.00	0.00	0.00	0.00
Total	100.71	98.50	100.71	99.60
Si	10.572	-	10.464	10.419
Al	5.394	-	5.499	5.553
Ca	1.468	-	1.600	1.540
Na	2.578	-	2.430	2.568
K	0.000	-	0.000	0.000
SUM CATS	20.012	-	19.993	20.080
Z	15.97	-	15.96	15.97
X	4.05	-	4.03	4.11
Ab	63.71	-	60.30	62.51
An	36.29	-	39.70	37.49
Or	0.00	-	0.00	0.00

Sample	S18	S18	S18	S18
Analysis	0015	0016	0017	0018
Location	CORE	RIM	CORE	RIM
Mineral	PLA	PLA	PLA	PLA
SiO2	61.23	60.89	58.98	60.58
Al2O3	25.29	24.28	26.18	25.07
CaO	6.52	6.27	7.88	6.55
Na2O	8.16	8.72	7.41	8.35
K2O	0.00	0.00	0.00	0.00
Total	101.20	100.16	100.45	100.55
Si	10.761	10.832	10.492	10.734
Al	5.235	5.087	5.485	5.231
Ca	1.228	1.195	1.502	1.244
Na	2.781	3.008	2.556	2.869
K	0.000	0.000	0.000	0.000
SUM CATS	20.004	20.121	20.035	20.077
Z	16.00	15.92	15.98	15.97
X	4.01	4.20	4.06	4.11
Ab	69.37	71.56	62.99	69.76
An	30.63	28.44	37.01	30.24
Or	0.00	0.00	0.00	0.00

Sample	S18	S18
Analysis	0019	0020
Location	CORE	RIM
Mineral	PLA	PLA
SiO2	61.32	60.07
Al2O3	25.02	25.16
CaO	6.55	6.56
Na2O	8.17	8.30
K2O	0.00	0.00
Total	101.06	100.09
Si	10.792	10.696
Al	5.186	5.276
Ca	1.235	1.252
Na	2.788	2.866
K	0.000	0.000
SUM CATS	20.001	20.090
Z	15.98	15.97
X	4.02	4.12
Ab	69.30	69.60
An	30.70	30.40
Or	0.00	0.00

Appendix C Chemical Data for Biotite

Sample	S1	S1	S10	S10
Analysis	0005	0006	0001	0002
Location	CORE	RIM	CORE	RIM
Mineral	BIO	BIO	BIO	BIO
SiO2	35.90	35.41	34.77	34.82
TiO2	3.16	2.71	3.35	3.72
Al2O3	15.72	15.92	16.86	16.42
FeO	18.50	19.05	18.94	19.28
MnO	0.34	0.32	0.31	0.26
MgO	10.35	10.48	9.94	9.51
CaO	0.00	0.00	0.00	0.00
Na2O	0.07	0.06	0.10	0.05
K2O	9.99	9.92	9.80	9.64
F	0.28	0.27	0.25	0.30
Cl	0.04	0.05	0.10	0.12
Total	94.35	94.19	94.42	94.12
-O=F	0.13	0.12	0.13	0.15
-O=Cl	0.13	0.12	0.13	0.15
-O=F,Cl	0.13	0.12	0.13	0.15
CTotal	94.22	94.07	94.29	93.97

Sample	S10	S10	S10	S10
Analysis	0003	0004	0020	0021
Location	CORE	CORE	CORE	RIM
Mineral	BIO	BIO	BIO	BIO
SiO2	35.12	35.47	36.44	36.53
TiO2	3.04	2.87	2.51	2.61
Al2O3	17.42	16.80	17.31	17.17
FeO	19.57	19.78	18.99	19.28
MnO	0.29	0.36	0.32	0.30
MgO	10.04	9.87	10.53	10.19
CaO	0.03	0.00	0.00	0.00
Na2O	0.09	0.07	0.03	0.04
K2O	9.77	9.97	9.80	9.84
F	0.38	0.25	-	-
Cl	0.14	0.10	-	-
Total	95.89	95.54	95.93	95.96
-O=F	0.19	0.13	0.00	0.00
-O=Cl	0.19	0.13	0.00	0.00
-O=F,Cl	0.19	0.13	0.00	0.00
CTotal	95.70	95.41	95.93	95.96

Sample	S10	S10	S11	S11
Analysis	0022	0023	0010	0011
Location	CORE	RIM	CORE	RIM
Mineral	BIO	BIO	BIO	BIO
SiO2	35.15	35.77	35.25	35.35
TiO2	2.63	2.54	2.76	2.65
Al2O3	16.96	17.35	16.68	16.62
FeO	19.54	18.39	19.83	19.26
MnO	0.31	0.29	0.30	0.23
MgO	10.47	10.36	9.66	10.11
CaO	0.00	0.00	0.00	0.00
Na2O	0.05	0.06	0.06	0.06
K2O	9.84	9.99	10.24	10.01
F	-	-	0.28	0.29
Cl	-	-	0.13	0.11
Total	94.95	94.75	95.19	94.69
-O=F	0.00	0.00	0.15	0.15
-O=Cl	0.00	0.00	0.15	0.15
-O=F,Cl	0.00	0.00	0.15	0.15
CTotal	94.95	94.75	95.04	94.54

Sample	S11	S11	S11	S13
Analysis	0012	0013	0014	0041
Location	CORE	RIM	CORE	CORE
Mineral	BIO	BIO	BIO	BIO
SiO2	34.18	35.32	34.23	35.67
TiO2	2.69	2.61	2.75	2.54
Al2O3	16.95	17.11	17.11	16.60
FeO	19.70	19.35	19.99	18.77
MnO	0.30	0.28	0.28	0.29
MgO	9.89	10.09	9.85	10.18
CaO	0.00	0.01	0.00	0.03
Na2O	0.05	0.04	0.07	0.08
K2O	10.04	9.97	9.98	9.64
F	0.32	0.31	0.25	0.28
Cl	0.14	0.11	0.12	0.11
Total	94.26	95.20	94.63	94.19
-O=F	0.17	0.16	0.13	0.14
-O=Cl	0.17	0.16	0.13	0.14
-O=F,Cl	0.17	0.16	0.13	0.14
CTotal	94.09	95.04	94.50	94.05

Sample	S13	S14	S14	S14
Analysis	0043	0024	0025	0027
Location	CORE	CORE	RIM	RIM
Mineral	BIO	BIO	BIO	BIO
SiO2	35.72	34.66	35.44	35.90
TiO2	2.80	2.97	2.91	1.97
Al2O3	16.57	16.57	16.12	16.89
FeO	19.22	19.04	19.38	19.04
MnO	0.35	0.38	0.36	0.30
MgO	10.01	10.06	9.80	10.29
CaO	0.00	0.00	0.00	0.00
Na2O	0.06	0.06	0.06	0.08
K2O	9.73	9.88	9.88	9.81
F	0.32	0.34	0.34	0.31
Cl	0.11	0.15	0.14	0.15
Total	94.89	94.11	94.43	94.74
-O=F	0.16	0.18	0.17	0.16
-O=Cl	0.16	0.18	0.17	0.16
-O=F,Cl	0.16	0.18	0.17	0.16
CTotal	94.73	93.93	94.26	94.58

Sample	S14	S14	S16	S16
Analysis	0028	0029	0037	0039
Location	CORE	RIM	CORE	CORE
Mineral	BIO	BIO	BIO	BIO
SiO2	35.50	36.24	35.74	35.52
TiO2	3.00	1.48	2.80	2.84
Al2O3	16.03	17.06	16.09	16.02
FeO	19.67	19.34	19.67	19.32
MnO	0.27	0.28	0.30	0.28
MgO	9.79	10.70	9.86	9.91
CaO	0.00	0.04	0.00	0.00
Na2O	0.09	0.06	0.05	0.06
K2O	9.99	9.78	9.67	9.96
F	0.28	0.31	0.27	0.28
Cl	0.13	0.16	0.13	0.12
Total	94.75	95.45	94.58	94.31
-O=F	0.15	0.17	0.14	0.14
-O=Cl	0.15	0.17	0.14	0.14
-O=F,Cl	0.15	0.17	0.14	0.14
CTotal	94.60	95.28	94.44	94.17

Sample	S17	S17	S17	S17
Analysis	0008	0009	0011	0013
Location	CORE	RIM	CORE	CORE
Mineral	BIO	BIO	BIO	BIO
SiO2	36.57	36.15	35.39	37.20
TiO2	3.14	2.71	3.03	2.13
Al2O3	16.38	16.66	16.73	16.60
FeO	19.18	19.47	19.40	19.00
MnO	0.32	0.30	0.35	0.33
MgO	10.07	10.03	9.87	11.00
CaO	0.00	0.01	0.00	0.00
Na2O	0.05	0.05	0.05	0.06
K2O	9.80	9.69	9.57	9.94
F	-	-	-	-
Cl	-	-	-	-
Total	95.51	95.07	94.39	96.26
-O=F	0.00	0.00	0.00	0.00
-O=Cl	0.00	0.00	0.00	0.00
-O=F,Cl	0.00	0.00	0.00	0.00
CTotal	95.51	95.07	94.39	96.26

Sample	S17	S17	S17	S17
Analysis	0014	0015	0016	0017
Location	RIM	CORE	RIM	RIM
Mineral	BIO	BIO	BIO	BIO
SiO2	35.77	35.50	35.88	36.87
TiO2	3.45	2.56	1.80	2.45
Al2O3	16.00	16.01	16.51	16.58
FeO	19.54	20.24	20.79	18.24
MnO	0.41	0.33	0.31	0.34
MgO	9.76	10.24	10.02	11.08
CaO	0.00	0.04	0.00	0.00
Na2O	0.03	0.05	0.05	0.04
K2O	9.76	9.52	9.68	9.81
F	-	-	-	-
Cl	-	-	-	-
Total	94.72	94.49	95.04	95.41
-O=F	0.00	0.00	0.00	0.00
-O=Cl	0.00	0.00	0.00	0.00
-O=F,Cl	0.00	0.00	0.00	0.00
CTotal	94.72	94.49	95.04	95.41

Sample	S17	S17	S17	S17
Analysis	0020	0021	0022	0023
Location	CORE	RIM	CORE	CORE
Mineral	BIO	BIO	BIO	BIO
SiO2	36.17	35.92	36.32	36.47
TiO2	2.36	0.84	2.76	2.71
Al2O3	16.07	16.94	16.12	16.17
FeO	19.01	18.43	19.02	19.22
MnO	0.36	0.33	0.33	0.38
MgO	10.71	11.57	10.59	10.42
CaO	0.00	0.00	0.00	0.02
Na2O	0.04	0.05	0.06	0.04
K2O	9.60	9.70	10.14	10.04
F	0.30	0.33	0.28	0.28
Cl	0.11	0.17	0.14	0.12
Total	94.73	94.28	95.76	95.87
-O=F	0.15	0.18	0.15	0.14
-O=Cl	0.15	0.18	0.15	0.14
-O=F,Cl	0.15	0.18	0.15	0.14
CTotal	94.58	94.10	95.61	95.73

Sample	S18	S18	S4	S4
Analysis	0032	0033	0044	0045
Location	CORE	RIM	CORE	RIM
Mineral	BIO	BIO	BIO	BIO
SiO2	36.14	35.38	36.12	36.08
TiO2	2.82	2.58	2.94	3.23
Al2O3	15.82	16.43	15.39	15.84
FeO	19.39	19.06	19.80	19.67
MnO	0.24	0.32	0.31	0.31
MgO	10.29	10.01	10.36	10.15
CaO	0.00	0.00	0.00	0.00
Na2O	0.05	0.07	0.06	0.04
K2O	9.83	10.32	9.91	9.31
F	0.32	0.27	0.29	0.37
Cl	0.08	0.09	0.13	0.13
Total	94.98	94.53	95.31	95.13
-O=F	0.15	0.13	0.15	0.19
-O=Cl	0.15	0.13	0.15	0.19
-O=F,Cl	0.15	0.13	0.15	0.19
CTotal	94.83	94.40	95.16	94.94

Sample	S4	S4	S5	S5
Analysis	0046	0048	0015	0016
Location	CORE	RIM	CORE	RIM
Mineral	BIO	BIO	BIO	BIO
SiO2	34.99	35.96	35.90	35.35
TiO2	3.48	3.55	2.82	2.59
Al2O3	15.55	15.84	16.16	16.05
FeO	20.15	20.13	18.69	19.50
MnO	0.28	0.29	0.30	0.36
MgO	9.92	9.65	10.66	10.36
CaO	0.00	0.00	0.00	0.03
Na2O	0.08	0.04	0.05	0.04
K2O	9.40	9.90	9.95	9.63
F	0.33	0.31	0.26	0.27
Cl	0.15	0.13	0.10	0.10
Total	94.33	95.80	94.89	94.28
-O=F	0.17	0.16	0.13	0.14
-O=Cl	0.17	0.16	0.13	0.14
-O=F,Cl	0.17	0.16	0.13	0.14
CTotal	94.16	95.64	94.76	94.14

Sample	S5	S5
Analysis	0017	0019
Location	CORE	CORE
Mineral	BIO	BIO
SiO2	36.47	36.01
TiO2	2.14	3.25
Al2O3	16.24	15.53
FeO	19.33	19.94
MnO	0.30	0.30
MgO	10.74	10.48
CaO	0.00	0.00
Na2O	0.04	0.06
K2O	9.77	9.74
F	0.34	0.30
Cl	0.11	0.10
Total	95.48	95.71
-O=F	0.17	0.15
-O=Cl	0.17	0.15
-O=F,Cl	0.17	0.15
CTotal	95.31	95.56

References

de Albuquerque CAR (1979) Origin of plutonic mafic rocks of southern Nova Scotia. Geol Soc Am Bull 90:719-731

Arzi AA (1978) Critical phenomena in the rheology of partially melted rocks. Tectonophysics 44:173-184

Barriere M (1981) On curved laminae, graded layers, convection currents and dynamic crystal sorting in the Ploumanac'h (Brittany) subalkaline granite. Contrib Min Petrol 77:214-224

Bowen NL (1928) in The Evolution of Igneous Rocks Princeton University Press 334p.

Burg JP, Ponce De Leon MI (1985) Pressure-solution structures in a granite. Jour Struct Geol 7:431-436

Castro A (1986) structural pattern and ascent model in the Central Extremadura batholith, Hercynian Belt, Spain

Dallmeyer RD and Keppie JD (1986) Polyphase late Paleozoic tectonothermal evolution of the Meguma Terrane, Nova Scotia Geol Soc Am Programs-With-Abstracts 18:11

Den Tex E (1969) Origin of ultramafic rocks, their tectonic setting and history: A conttribution to the discussion of the

paper " The origin of ultramafic and ultrabasic rocks" by P.J Wyllie. Tectonophysics 7:457-458

Frost TP, Mahood GA (1987) Field, chemical and physical contraints on mafic-felsic interaction in the Lamarck Granodiorite, Sierra Nevada, California. Geol Soc. Am. Bull 99:272-291

Hutton DHW, Dempster TJ, Brown PE, Becker SD (1990) A new mechanism of granite emplacement: intrusion in active extensional shear zones. Nature 343:452-455

Marre J (1986) The structural analysis of granitic rocks Elsevier New York

Paterson SR, Vernon RH, Tobisch OT (1988) A review of criteria for the identification of magamtic and tectonic foliations. Jour Struct Geol 11:343-363

Paterson SR, Tobish OT, Vernon RH (1989) Criteria for establishing the relative timing of pluton emplacement and regional deformation. Geology May 474-476

Pitcher WS, Berger AR (1972) The geology of Donegal Wiley Interscience New York

Reynolds PH et al. (1987) Thermal history of the southwestern

Meguma Zone, Nova Scotia, from an Ar/Ar and fission track dating study of intrusive rocks. Can J Earth Sci 24:1952-1965

Rogers HD (1986) geology and igneous petrology of Shelburne and Eastern Yarmouth Counties, Nova Scotia unpublished MSc Thesis, Acadia University

Rogers HD, Barr SM (1988) Petrology of the Shelburne and Barrington Passage plutons, southern Nova Scotia. Marit Sed Atlant Geol 24:21-31

Streckeisen A (1976) To each plutonic rock its proper name Earth Sci Rev 12:1-33

Zen E, Hammarstrom JM (1984) Magmatic epidote and its petrologic significance Geology 12:515-518